Title: Dynamics of ecosystem carbon balance recovering from a clear-cutting in a cool-temperate forest

Authors:

Maricar Aguilos[1](mmaguilos@yahoo.com), Kentaro Takagi[2*](kentt@fsc.hokudai.ac.jp), Naishen Liang[3](liang@nies.go.jp), Masahito Ueyama[4](miyabi-flux@muh.biglobe.ne.jp), Karibu Fukuzawa[2](caribu@fsc.hokudai.ac.jp), Mutsumi Nomura[2](nomu@fsc.hokudai.ac.jp), Osamu Kishida[2](kishida@fsc.hokudai.ac.jp), Tatsuya Fukazawa[5](tatsuya@eng.hokudai.ac.jp), Hiroyuki Takahashi[2](frsthiro@fsc.hokudai.ac.jp), Chikara Kotsuka[2](ckozuka@fsc.hokudai.ac.jp), Rei Sakai[2](reisakai@fsc.hokudai.ac.jp), Kinya Ito[2](kinya-i@fsc.hokudai.ac.jp), Yoko Watanabe[2](youko@for.agr.hokudai.ac.jp), Yasumi Fujinuma[6](fujinuma@kankyo-u.ac.jp), Yoshiyuki Takahashi[3](yoshiyu@nies.go.jp), Takeshi Murayama[7](murayama@epmail.hepco.co.jp), Nobuko Saigusa[3](n.saigusa@nies.go.jp), and Kaichiro Sasa[2](sasa@fsc.hokudai.ac.jp)

[1]Graduate School of Environmental Science, Hokkaido University, Sapporo 060-0809, Japan

[2]Field Science Center for Northern Biosphere, Hokkaido University, Sapporo 060-0809, Japan

[3]Center for Global Environmental Research, National Institute for Environmental Studies, Tsukuba 305-0056, Japan

[4]School of Life and Environmental Science, Osaka Prefecture University, Sakai 559-8531, Japan

[5]Graduate School of Engineering, Hokkaido University, Sapporo 060-8628, Japan

[6]Department of Environmental Management, Tottori University of Environmental Studies, Tottori, 689-1111 Japan

[7]*Research and Development Department, Hokkaido Electric Power Co., Inc., Ebetsu, 067-0033, Japan*

[*]**Author for correspondence:**

Kentaro Takagi

Teshio Experimental Forest, Field Science Center for Northern Biosphere,

Hokkaido University, Toikanbetsu, Horonobe, 098-2943 Japan

Phone: +81-1632-6-5211/Fax: +81-1632-6-5003

E-mail: kentt@fsc.hokudai.ac.jp

Type of paper: Original article

Abstract

A mixed forest in northern Japan, which had been a weak carbon sink (net ecosystem CO_2 exchange [NEE] = –0.44 ± 0.5 Mg C ha^{-1} yr^{-1}), was disturbed by clear-cutting in 2003 and was replaced with a hybrid larch (*Larix gmelinii* × *L. kaempferi*) plantation in the same year. To evaluate the impact of the clear-cutting on the ecosystem's carbon budget, we used 10.5 years (2001–2011) of eddy covariance measurements of CO_2 fluxes and the biomass observation for each ecosystem component. BIOME-BGC model was applied to simulate the changes in the carbon fluxes and stocks caused by the clear-cutting. After clear-cutting in 2003, the ecosystem abruptly became a large carbon source. The total CO_2 emission during the first 3 years after the disturbance (2003–2005) was 12.2 ± (0.9–1.5; possible min–max range of the error) Mg C ha^{-1}, yet gradually decreased to 2.5 ± (1–2) Mg C ha^{-1} during the next 4 years. By 2010, the ecosystem had regained its status as a carbon sink (NEE = –0.49 ± 0.5 Mg C ha^{-1} yr^{-1}). Total gross primary production, ecosystem respiration, and NEE during the 7 years after the clear-cutting (2003–2009) were 64.5 ± (2.6–7), 79.2 ± (2.6–7), and 14.7 ± (1.3–3.5) Mg C ha^{-1}, respectively. From 2003 to 2009, the understory *Sasa* biomass increased by 16.3 ± 4.8 Mg C ha^{-1}, whereas the newly planted larch only gained 1.00 ± 0.02 Mg C ha^{-1}. The BIOME-BGC simulated observed carbon fluxes and stocks, although further modification on the parameter set may be needed according with the tree growth and corresponding suppression of *Sasa* growth. Ecosystem carbon budget evaluation and the model simulation suggested that the litter including harvest residues became a large carbon emitter (~31.9 Mg C ha^{-1}) during the same period. Based on the cumulative NEE during the period when the forest was a net carbon source, we estimate that the ecosystem will require another 8 to 34 years to fully recover all of the CO_2 that was emitted after the clear-cutting, if off-site carbon storage in forest products is not considered.

59

60 **Key words:** BIOME-BGC; carbon budget; carbon compensation point; clear-cutting; forest
61 disturbance; *Sasa*

62

1. Introduction

The anthropogenic land cover change constitutes a source of emissions mainly from the loss of terrestrial biomass, and Houghton (2003) estimated that ca. one third of the anthropogenic CO_2 emissions over the last 150 years is considered to be the direct consequence of land use changes. Clear-cut harvesting is one of the important type of forest management, and understanding how this form of logging affects a site's carbon balance is critical not only for determining appropriate carbon management scenarios of forests, but also for including such effect into global carbon cycling models to obtain better prediction (Pongratz et al., 2009). However, accurate quantification of wood harvesting effects on the carbon dynamics including harvest residues and belowground carbon dynamics is still lacking (Howard et al., 2004; Noormets et al., 2012).

Clear-cutting removes the commercial stem wood and leaves residues (foliage, twigs, branches, stumps, and roots) on the site. It eliminates canopy photosynthesis and affects autotrophic and heterotrophic respiration both directly and indirectly. As a result, the post-harvest stand is expected to be a net source of carbon for several years after disturbance (Kolari et al., 2004; Amiro et al., 2006; Humphreys et al., 2006; Zha et al., 2009; Grant et al., 2010; Goulden et al., 2011; Noormets et al., 2012). The ecosystem carbon compensation point is the time when stands regain their role as a carbon sink by regenerating after a harvest or a similarly severe disturbance. It is a critical index to characterize the carbon budget of a managed forest (Kowalski et al., 2004). For example, it takes a warm template plantation 3 years (Clark et al., 2004) or boreal forests 7–20 years (Bond-Lamberty et al., 2004; Howard et al., 2004; Kolari et al., 2004; Freeden et al., 2007; Amiro et al., 2010) to recover from carbon source to sink. Another critical index is the payback period before the forest recaptures as much CO_2 as was

emitted during the recovery period, however quantitative evaluation of these indexes based on the long-term observation is still a challenge.

Carbon dynamics of forest ecosystems can be investigated by using the eddy covariance method (Mission et al., 2005; Giasson et al., 2006; Amiro et al., 2010). Previous studies often use sites of different ages in parallel to infer the status of an ecosystem as a function of the time since disturbance (Amiro et al., 2010; Goulden et al., 2011). However, it is difficult to judge whether the sites of different ages are following the same trajectory (Walker et al., 2010). In addition, estimating the total carbon emission during the period when the forest was a net carbon source, which is an important factor that determines the magnitude of a disturbance and the payback period, is difficult when dealing with such chronosequence studies because of the gaps in the CO_2 flux data among the measurements at different stands for several years within the chronosequence.

To obtain a complete series of pre- and post-harvest NEE data until a disturbed ecosystem reached its carbon compensation point (i.e., until it once more became a net carbon sink), we conducted an experimental clear-cutting and plantation establishment study in a cool-temperate mixed forest in northern Japan. Using the eddy covariance method, we started our measurements 1.5 years prior to clear-cutting and continued for 9 years after harvesting to shed light on several doubts that are raised by chronosequence studies. In addition, the BIOME-BGC model (Kimball et al., 1997a, b) was applied to simulate these characteristics and to complement the change in the carbon stocks in the soil and litter compartments. This model is widely applied to many types of terrestrial ecosystems and succeeds in simulating the carbon cycles with substantial information on each parameter values (White et al., 2000; Pietsch et al., 2005). The model has

been successfully applied in simulating the disturbance effects on the cycles (Thornton et al., 2002).

Our focus was to determine the carbon budget during the dramatic shifts that occur during the forest transitions from a sink to a source and back again to a sink, total CO_2 emission into the atmosphere during the period when the forest was a net carbon source, and the estimated payback period before the forest recaptures as much CO_2 as was emitted during the recovery period. The results from the first 5 years (2001 to 2005) of the assessment were reported by Takagi et al. (2009) and revealed the shift of the ecosystem from a carbon sink to a carbon source. In the present paper, we added the subsequent 6 years (2006 to 2011) data to document the transition from a carbon source to a carbon sink and to discuss the ecosystem carbon compensation caused by clear-cutting.

2. Methods

2.1. Site description and management

The study site lies on a flat terrace inside the Teshio Experimental Forest of Hokkaido University (45°03'N, 142°06'E, 66 m a.s.l.). Its soil, mainly a Gleyic Cambisol, has a surface organic horizon that is about 10 cm thick. Prior to clear-cutting, the forest was a naturally regenerated mature forest in the late successional stage and large trees were more than 200-years old (Tsuji et al., 2006), although a Blizzard caused a severe tree-fall damage in December 1972. The dominant tree species were *Quercus crispula* Blume, *Betula ermanii* Cham., *Abies sachalinensis* (F. Schmidt) Mast., and *Betula platyphylla* var. *japonica* (Miq.) Hara. Maximum and mean tree heights were 24 and 20 m, respectively. The forest floor was covered with dense evergreen dwarf bamboos (*Sasa senanensis* Rehd. and *Sasa kurilensis* (Rupr.) Makino *et* Shibata). The plant area index (PAI) values for the canopy trees and the *Sasa* bamboos, measured using an LAI-2000 leaf-area meter (Li-Cor, Lincoln, NE, USA), were 3.2 and 4.1 m^2 m^{-2}, respectively, at this parameter's seasonal maximum in 2002 (Fig. 1). From January to March 2003, trees covering an area of 13.7 ha were clear-cut. The total biomass volume of trees at the site was 2193 m^3 (Koike et al., 2001), of which 1203 m^3 (ca. 25 Mg C ha^{-1}) were removed as logs.

Sasa was left intact under the snowpack, but 7 months later, just before the planting of hybrid larch seedlings (in late October 2003), they were strip-cut into alternating 4-m-wide cut and uncut rows in the clear-cut area to give space for the planting of ca 30 000 2-year-old hybrid larch (*Larix gmelinii* (Rupr.) Kuzen. ver *japonica* (Maxim. Ex Regel) Pilg. × *L. kaempferi* (Lamb.) Carrière) at a density of 2500 ha^{-1} (0.04 Mg C ha^{-1}). In the rows where *Sasa* remained, *Sasa* PAI increased steeply from 1 year after clear-cutting until 2007, reaching a peak at 8.0 m^2 m^{-2} in 2010, which is about double the value in 2002 before clear-cutting. In the rows where

143 *Sasa* was strip-cut, *Sasa* weeding was conducted from once (2005 and 2006) to three times
144 (2004) per year between late May and late July to eliminate all *Sasa* growing between the larch
145 trees. The *Sasa* was no longer weeded starting in 2007 because the larch was higher than the
146 surrounding *Sasa*, and was able to receive enough solar radiation to grow without interference.
147 *Sasa* soon recovered in the strip-cut rows, and in 2008, 2 years after the last weeding, the PAI
148 was almost the same as that in the surrounding uncut rows, blanketing all gaps between the trees.
149 On the other hand, the PAI of the larch remained low (1.7 m^2 m^{-2} in 2010) at its seasonal
150 maximum, lower than that of *Sasa*.
151
152 *2.2. The eddy covariance system*
153 A closed-path eddy covariance system was established in August 2001 on a 32-m-tall tower in
154 the mixed forest to evaluate the CO_2 fluxes. A sonic anemometer (DA600-3TV, Kaijo, Tokyo,
155 Japan) and an infrared gas analyzer (IRGA; LI-7000, Li-Cor, Lincoln, NE, USA) were used to
156 evaluate the fluxes. In addition, another closed-path system comprising the same instruments was
157 installed at a height of 4.6 m in October 2003 after clear-cutting, and the measurements were
158 continued until 2011. The height of the instruments was changed to 5.7 m in May 2007. In this
159 system, the separation distance between the anemometer and the air intake was 5 cm, and the air
160 was drawn into the system at a flow rate of 10 L min^{-1} through a 1.0-μm filter and into a 15-m
161 Teflon tube (6 mm in diameter). The IRGA reference cell was fed with CO_2 gas of known
162 concentration (300 μmol mol^{-1}) at a flow rate of 10 to 20 mL min^{-1}. The CO_2 concentration was
163 calibrated daily using two standard gases between 23:00 and 24:00 h. The data were sampled at a
164 frequency of 10 Hz with a digitizing data recorder (DRM3, TEAC Corp., Tokyo, Japan, until
165 October 2003; CR5000, Campbell Scientific, Logan, UT, USA, from October 2003) after low-

pass filtering (with a cut-off frequency of 5 Hz). Takagi et al. (2009) provided a more detailed description of the system, especially before 2006.

2.3. Micrometeorological measurements

Meteorological measurements at a height of 32 m included air temperature and relative humidity (HMP45A, Vaisala, Helsinki, Finland), wind speed and direction (010C and 020C, Met One Instruments, Grants Pass, OR, USA), and photosynthetic photon-flux density (PPFD; LI-190SZ, Li-Cor, until May 2007; ML-020P, EKO Instruments Co. Ltd., Tokyo, Japan, from May 2007). These parameters were also monitored above the *Sasa* canopy (~2 m above the ground) using the same type of instruments used at 32 m. Snow depth (SR-50, Campbell Scientific) and atmospheric pressure (PTB210-C6C5A, Vaisala) were also measured. Rainfall was measured using a tipping-bucket rain gauge (CYG-52202, RM Young, Traverse City, MI, USA) at a height of 32 m before clear-cutting and at a height of 3 m after clear-cutting. The soil temperature profile (at depths of 1, 5, and 10 cm below the soil surface) and the soil water content profile (at depths of 5 and 10 cm) were measured at five points using platinum resistance thermometers and time-domain-reflectometry sensors (CS615, Campbell Scientific), respectively. Calibration of the HMP45A and ML-020P sensors was conducted every year (in May) and the coefficients used to convert the measured value to the physical value were updated. The meteorological and soil data were sampled every 5 s, and data were stored as 0.5-h means using three dataloggers (two CR23Xs and one CR10X, Campbell Scientific) connected to a PC, which downloaded the logged data automatically.

2.4. Biomass measurements

A 50 × 50 m plot was established in 2000 to monitor the change in diameter at breast height (DBH) of all trees with DBH >6 cm until January 2003 in the mixed forest adjacent to the flux tower. The number and basal area of the trees in this plot were 155 and 21.8 m^2 ha^{-1} in April 2000. To evaluate the change in tree DBH during 2002, we used data obtained in April 2002 and January 2003. The following allometric equation was used to calculate the biomass increments from the DBH increments of all trees in the plot:

$$\ln Y = (2.250 \pm 0.084) \times \ln X_{\text{breast}} - (1.427 \pm 0.390) \quad (1),$$

where X_{breast} and Y represent DBH (cm) and whole-tree biomass including roots (kg), respectively. This equation was obtained by Takagi et al. (2010) from destructive sampling of 22 trees (*Q. crispula, B. ermanii,* and *A. sachalinensis*) around the study plot, ranging from 3.8 to 55 cm in DBH. Using this equation, we evaluated tree biomass and the possible maximum and minimum errors within the standard deviation for each tree in the plot, then the error of the total biomass (SE_{total}) was estimated as the square root of the sum of squares of the errors in each tree (Taylor, 1997) using equation (2), assuming that the uncertainty in each tree biomass evaluation (SE_i) was caused only by random errors.

$$SE_{\text{total}} = \sqrt{\sum_{i=1}^{n} (SE_i)^2} \quad (2)$$

Prior to clear-cutting, three 2 × 1 m plots were established in 2001 to evaluate the aboveground biomass of *Sasa* in shaded positions under the forest canopy and in illuminated positions below canopy gaps. The dry mass of each plant part (leaves and culms) was weighed after oven-drying at 80 ºC. A 0.5 × 0.5 m subplot was established in each of the six plots, and the

rhizome-roots of *Sasa*, including fine roots, were collected to a depth of 40 cm below the top of the organic layer, and the biomass was obtained.

Two 50 × 50 m plots were established in 2004 after clear-cutting to monitor the height and the basal diameter of every larch in the plot. The number of larch was 571 in the first plot and 549 in the second plot in October 2004. We measured the height and basal diameter annually between late October and early November until 2010. To estimate the biomass increment of the larch using the basal diameter increment, we conducted destructive sampling of 14 larch, ranging from 2.7 to 6.8 m in height, in August 2010. The whole-tree biomass including roots (Y; kg) was related to the basal diameter (X_{basal}; cm) using the following allometric equation:

$$\ln Y = (2.197 \pm 0.069) \times \ln X_{basal} - (2.698 \pm 0.187) \quad (3).$$

Error of all-tree biomass was estimated using the same procedure with that for trees before clear-cutting. Carbon content (g C) was estimated as half of the biomass (g DW) of all trees, *Sasa*, and larch.

2.5. Soil respiration measurements

We measured soil respiration (including both autotrophic and heterotrophic respiration) using a multichannel automated chamber system (based on the design of Liang et al. 2010) that was installed during snow-free periods from 2003 to 2009 after clear-cutting. As described by Takagi et al. (2009), the system included a control unit with an IRGA (LI-840, Li-Cor) and a datalogger (CR10X, Campbell Scientific), and it was used to monitor eight automated chambers (0.9 × 0.9 × 0.5 m high). In 2003, the CO_2 concentration was measured at 1-s intervals for 225 s for each of

the eight chambers within 0.5-h, and soil respiration rate was evaluated every 0.5-h for every chambers. In 2004 and 2005, the sampling period and respiration evaluation interval were changed to 150 s and 1 h, respectively. Since 2006, the CO_2 concentration was measured at 1-s intervals for 225 s in each chamber at 1-h intervals, and the 10-s averages from the last 160 s of these measurements were stored in the datalogger.

The soil respiration rate (R_s, μmol m^{-2} s^{-1}) was calculated as follows:

$$R_s = \frac{PV}{S\,R(T_c + 273.15)}\left(\frac{\partial C}{\partial t}\right) \qquad (4),$$

where V and S are the effective chamber head-space volume (0.405 m^3) and the measured soil surface area (0.81 m^2), respectively; R is the universal gas constant (8.134 J K^{-1} mol^{-1}), and P and T_c are the initial pressure (1013.25 hPa) and temperature (ºC) in the chamber, respectively; and $\partial C/\partial t$ is the rate of change of the CO_2 concentration over time (μmol mol^{-1} s^{-1}). In this study, air temperature observed at 2 m in height was used for T_c, instead of using the air temperature inside the chamber. This treatment causes < 2% overestimation even under a 5ºC difference between these temperatures. Low-quality R_s was removed by checking the stationarity of the $\partial C/\partial t$ according with the procedure proposed by Aguilos et al. (2013). Data gap ratio during whole snow-free period was 27.6±10.4% (average ± standard deviation of all years) after this procedure and quality-assured data still distributed over the wide range of temperature. Data gaps caused by system malfunctions or quality checking were filled using an Arrhenius-type equation (Lloyd and Taylor, 1994) for each chamber and each year:

$$R_s = R_{ref} \times \exp\left[\frac{E_a}{R} \times \left(\frac{1}{T_{ref}} - \frac{1}{T}\right)\right] \quad (5)$$

where R_{ref} is the respiration rate (μmol m^{-2} s^{-1}) at the reference temperature (T_{ref} =283.15 K); E_a is the apparent temperature sensitivity (or activation energy) (J mol^{-1}); and T is the temperature (K) as an independent variable for respiration (soil temperature at a depth of 5 cm). The constants E_a and R_{ref} were fixed throughout the year, and were determined using the least squares method (Table 1). The average (± standard deviation) of standard error of the estimated coefficients was 0.04±0.04 μmol m^{-2} s^{-1} (or 1.0±0.3%; the percentages of the error to the coefficients) for R_{ref} and 1.1±0.4 KJ mol^{-1} (2.2±3.6%) for E_a, thus showing strong temperature dependence of the soil respiration, and applicability of the regression with fixed coefficient during each snow-free period.

2.6. Eddy flux calculation

Following the same procedure used in the previous study at the site (Takagi et al., 2009), we determined the daily sonic rotation angle for use in the planar fit rotation (Wilczak et al., 2001) using the 30-min mean wind speed in a 15-day moving window. We determined the fixed value of the sonic-tube lag time for CO_2 monthly by averaging the lag times obtained at 30-min intervals under turbulent conditions. The range of monthly averages for lag time was 2.9 to 6.3 s (with an average of 4.2 s) at a height of 32 m and 2.7 to 4.6 s (with an average of 3.7 s) at heights of 4.6 or 5.7 m. Using these angles and lag times, half-hourly CO_2 fluxes (F_c, μmol m^{-2} s^{-1}) were calculated. We applied block averaging (30 min) but not detrending to the 10 Hz fluctuation data when we calculated the covariance to keep low frequency fluctuations (Moncrieff et al., 2004).

279 Crosswind speed and water vapor concentration effects on the sensible heat flux were corrected
280 using the methods of Kaimal and Gaynor (1991) and Hignett (1992), respectively, then we
281 corrected the effect of air density fluctuations on the flux values (Leuning and King, 1992).
282 High-frequency losses for the sonic sensor's span and sensor separation were corrected
283 using transfer functions related to the sources of signal damping (Moore, 1986), and losses for
284 tube attenuation were corrected following the method of Kowalski et al. (2003). Co-spectra
285 between the vertical winds and the scalars (temperature and CO_2 concentration) were normalized
286 by integrating the covariance over the band-pass range (0.003 to 0.01 Hz) and averaged over
287 periods with a similar wind speed under turbulent conditions. The correction factor (ε) was
288 determined from the ratio of the integrated, normalized co-spectra, using temperature as a
289 reference. ε depends on the mean wind speed ($\bar{u}$) based on the relationship $\varepsilon = a + b\bar{u}$, where a
290 and b are regression coefficients that were determined every year or after a change in the system;
291 a and b were 1.12 and 0.006, respectively in 2002 at a height of 32 m and 0.91 to 1.12 and 0.109
292 to 0.266, respectively, from 2003 to 2011 at heights of 4.6 or 5.7 m.
293 Before clear-cutting, NEE (μmol m^{-2} s^{-1}) was determined as the sum of F_c and F_s, where F_s
294 is the change in CO_2 storage in the air column from the forest floor to the flux measurement
295 height and was calculated from the observed CO_2 profiles measured at four (snow-covered
296 period) or five (snow-free period) levels with an IRGA (DX6100, RMT Ltd., Moscow, Russia)
297 (Takagi et al., 2009). After clear-cutting, F_c was used to represent NEE because the nighttime F_c
298 was stable when the friction velocity (u_*) exceeded 0.1 m s^{-1}.
299
300 *2.7. Quality control, gap filling for NEE, and flux partitioning*

In checking the raw flux data, we followed the quality control program developed by Vickers and Mahrt (1997) and Mano et al. (2007). We applied instationarity ratio and integral turbulence characteristic tests (Foken and Wichura, 1996) to the 30-min averaged flux data. To remove the effect of fluxes from outside the clear-cut, we evaluated the footprint of the observed CO_2 flux using the model developed by Kormann and Meixner (2001). We evaluated the cumulative footprint every 30 min up to a distance of 2 km and up to the boundaries of the cut area (over a distance ranging from 140 to 340 m, depending on the wind direction) from the observation point in 1-m steps. The flux data were removed if the ratio of the two cumulative values was <0.7.

u_* filtering was applied to the remaining NEE data. As the threshold values for the filtering, we used 0.3 and 0.1 m s^{-1} for the forest and clear-cut, respectively; however, during the snow-covered period after clear-cutting, filtering was not applied (Takagi et al., 2005a, 2009). Using this quality-control procedure, we rejected about half of the 30-min NEE values each year.

We have also conducted continuous latent heat flux monitoring using open-path CO_2/H_2O analyzer (LI-7500, Li-Cor) from 2007 (Takagi, 2012). The average and the standard deviation of the energy balance ratio (ratio of the cumulative sum of half-hourly (H+lE) to (R_n-G-S)) during each snow-free period of each year was 0.74±0.03 for the last 5 years from 2007 to 2011. Here, H, lE, R_n, G and S is the sensible heat flux, latent heat flux, net radiation, soil heat flux, and heat storage flux in the soil surface layer, respectively. The ratio is not high and suggests the possibility of the systematic underestimation of the evaluated fluxes, although our value is close to the mean (0.79±0.01) of previous studies (Wilson et al., 2002).

We mainly used a lookup table to fill in the gaps in NEE (Falge et al., 2001). For each year, lookup tables were created every 30 days during snow-free periods, and another table was prepared for the snow-covered period. During the snow-free periods, air temperature and PPFD

were used as the environmental factors to create the lookup tables both before and after clear-cutting. During the snow-covered period, air (forest) or soil (clear-cut) temperatures and wind speeds were used to create the lookup tables. Some data gaps (<5% of the set of 30-min data in a year) after applying the lookup tables were filled using the mean diurnal variation approach (Falge et al., 2001), in which missing NEE was replaced by the mean for that time based on the adjacent 9 days. The few remaining gaps (<1% of the total) were filled by means of linear interpolation.

Night-time NEE (PPFD < 1 μmol m^{-2} s^{-1}) during the snow-free period and NEE during the snow-covered period were assumed to be equivalent to ecosystem respiration (RE) (i.e. gross primary production (GPP) was assumed to be 0). During the snow-free period, the 30-min values of night-time NEE were compiled for air temperature classes (2°C intervals), and the average NEE for each temperature class was related to the air temperature using equation (5) for each year. The constants R_{ref} and E_a were fixed throughout a given snow-free period (Table 1), and daytime RE was estimated every 30 min using the equation (5) and air temperature with determined R_{ref} and E_a. Half-hourly GPP was estimated as RE – NEE. However, estimated half-hourly GPP or RE sometimes shows unrealistic negative values originated from the random scatter in the NEE during snow-free period (negative RE) or from the higher NEE than RE during the transition period from snow-covered to snow-free period and vice versa (negative GPP), although the magnitude was small. Thus, we set the minimum time resolution for GPP or RE as the daily sum, and if the daily GPP (or RE) was still negative, the value was set to zero and the absolute value of the negative value was added to the daily RE (or GPP). This treatment changed the annual GPP and RE values only by 1±1% during the 10-year observation, removing all unrealistic negative daily GPP and RE with no change in the observed daily NEE value.

Takagi et al. (2009) evaluated the possible errors included in the estimates of annual NEE, GPP, and RE by comparing with other gap-filling and flux partitioning procedures proposed by Reichstein et al. (2005) and Hirata et al. (2008), and concluded that the error was about 0.5 Mg C ha^{-1} for annual NEE, versus about 1 Mg C ha^{-1} for the annual GPP and RE. If this uncertainty was caused only by random errors, the *n*-year total error (SE_{total}) in the carbon flux can be estimated using equation (2) as the square root of the sum of squares of the errors in each year (SE_i) . On the other hand, if the uncertainty in the annual sums was caused only by systematic errors, the *n*-year total error can be evaluated as the sum of the annual errors during the period. Thus, we express the possible errors in the cumulative flux at the *n* th year as the range of the two extreme cases.

2.8. BIOME-BGC model

Change in the carbon balance caused by clear-cutting was simulated using BIOME-BGC model (ver. 4.2: Thornton et al., 2002). The model has three compartments for carbon and nitrogen: vegetation, litter, and soil. Each compartment is sub-divided into four-pools based on the differences in their function (*e.g*. leaf, stems, coarse roots, and fine roots) and residence time (*e.g*. active, intermediate, slow, and passive recycling). GPP is estimated by coupling the Farquhar biochemical model (Farquhar et al., 1980) with the stomatal conductance model (Jarvis, 1976). RE is calculated as the sum of autotrophic and heterotrophic respiration (AR and HR, respectively). The AR and HR are calculated from the carbon and nitrogen pools and the temperature (for AR and HR) and soil water condition (for HR only). Further details for the BIOME-BGC model have been described in previous papers (Kimball et al., 1997a, b; White et al., 2000; Thornton et al., 2002; Ueyama et al., 2009).

The model was initialized by a spinup run for 1050 years, in which the dynamic equilibrium of the soil organic matter was determined by using a constant CO_2 concentration of 280 ppm and the observed daily meteorological data from 1962 to 2011. From 1962 to 2001, we used daily meteorological data observed at Wakkanai (52 km far from the study site) or Teshio (35 km) by Japan Meteorological Agency, and meteorological data observed at the study site were used from 2002 to 2011. Initial snowpack and soil water content were set as 500 kg m^{-2} and 50%, respectively. N deposition was fixed at 0.001 kgN m^{-2} $year^{-1}$ throughout the spinup run and the following simulation. We used Deciduous–C3–Woody species mode and specified the phenology, and referred parameters proposed by Pietsch et al. (2005) for *Quercus robur/petraea* (deciduous) forest, with minor adjustments on the parameters to reproduce the observed carbon fluxes and storages (Table 2).

The study site experienced severe tree-fall damage by a Blizzard in December 1972. There was no available forest biomass or stand volume data before the disturbance. However based on the information on the timbers transferred out from the site (226 m^3 ha^{-1}) after the disturbance and stand volume (400–500 m^3 ha^{-1}) of well developed forest around this region (Takahashi et al., 2006), all the plant carbon and nitrogen pools were decreased by 50% in 1973 to simulate the forest disturbance in the model, in accordance with the harvesting protocols proposed by Thornton et al. (2002). Then the carbon budget from 1974 to 2002 was simulated using observed climate (same with the data set for spinup run) and CO_2 concentration data, and same parameters set used for the spinup run. From 1974 to 2001, we used CO_2 data published by Enting et al. (1994) and Tans and Conway (2005), and observed concentration at the study site were used for 2002.

In 2003, all the plant carbon and nitrogen pools were decreased by 80% to apply the clearcut harvesting in the model. Because the half of the undergrowth *Sasa* (6–13 Mg C ha^{-1}) was kept intact during harvesting and strip-cutting, although all trees in the study site (63 Mg C ha^{-1} for the above-ground biomass) were clear-cut, we set the affected proportion at 80% instead of 100%. The affected proportion of the leaf and fine root carbon and nitrogen pools was sent to the fine litter, and the affected proportion of below ground live and dead wood carbon and nitrogen pools was sent to the CWD pools as the protocol (Thornton et al., 2002). However, 40% of carbon (29 of 73 Mg C ha^{-1}) and nitrogen (80 of 199 kgN ha^{-1}) of the affected proportion of above ground live and dead wood carbon and nitrogen pools was sent to 2 litter pools (22 Mg C ha^{-1} to litter 3 (shielded cellulose) and 7 Mg C ha^{-1} to litter 4 (Lignin) carbon pools, and 60 kgN ha^{-1} to litter 3 and 20 kgN ha^{-1} to litter 4 nitrogen pools), although Thornton et al. (2002) assumed that the affected proportion of aboveground live and dead wood carbon and nitrogen pools are removed from the site, and no longer enter into the site mass balance. This is because this portion of fallen trees (small woods and branches) was remained in the study site as residuals. The carbon budget from 2003 to 2011 after clear-cutting was simulated using observed climate and CO_2 concentration data and a new set of parameters (Table 2) after these translocations of carbon and nitrogen pools. Each parameter was adjusted considering the specific features of the clearcut ecosystem (e.g. large contribution of *Sasa* dwarf bamboo to the ecosystem carbon and nitrogen cycles). *Sasa* behaves like a perennial grass or shrub in the carbon and nitrogen cycle of the ecosystem, and we simulated the features by adjusting the parameters for allocation and turnover rate of each organ, canopy light extinction coefficient, specific leaf area, N content in Rubisco, and stomatal and boundary layer conductances. We used “deciduous mode” because larch is a deciduous tree and whole the evergreen *Sasa* canopy is under the snowpack in winter.

415 We set slightly higher value for the whole-plant mortality fraction considering the *Sasa* weeding
416 during 2004 to 2006.
417

3. Results

3.1. Interannual variation of carbon fluxes under a series of forest management

The mixed forest was a weak carbon sink (–0.44 Mg C ha^{-1} yr^{-1}) before logging (Takagi et al., 2009). After clear-cutting in 2003, large net carbon emission occurred due to the large decline in GPP. The total CO_2 emission during the first 3 years after the clear-cutting (2003–2005) was 12.2± (0.9–1.5; possible min–max range of the error) Mg C ha^{-1} (Fig. 2 and Table 3). The large emission rate decreased sharply with increasing GPP. From 2006 to 2009, GPP and RE showed similar rates compared with previous years and the total CO_2 emission was 2.5± (1–2) Mg C ha^{-1} during the 4 years. The ecosystem was a net carbon source on an annual basis until 2009. In 2010, the ecosystem regained its status as a net carbon sink (–0.49 Mg C ha^{-1} yr^{-1}) and the similar NEE (–0.52 Mg C ha^{-1} yr^{-1}) was observed in the following year. The magnitude was similar to that obtained in 2002 by the mixed forest.

Remarkable increase in NEE was observed shortly after clear-cutting (Fig. 2). However, the rate of CO_2 release gradually decreased until 2006, and by the end of 2010, NEE had largely stabilized due to the combination of a more or less stable ecosystem respiration rate and increasing GPP. GPP, RE, and NEE totaled 64.5± (2.6–7; possible min–max range of the error), 79.2± (2.6–7), and 14.7± (1.3–3.5) Mg C ha^{-1}, respectively, during the 7 years from 2003 to 2009 after the clear-cutting and before the transition of the forest into a net carbon sink. The total carbon transported out of the forest as logs by clear-cutting equaled ca. 25 Mg C ha^{-1}, thus the carbon loss as CO_2 emission during the 7 years (14.7 Mg C ha^{-1}) equaled 59 % of the carbon loss as logs, and 37% of total carbon loss (logs plus NEE = 39.7 Mg C ha^{-1}) from the ecosystem as a result of the clear-cutting.

Clear-cutting decreased both GPP and RE at the same air temperature, however the decrease in GPP was larger than RE (Fig. 3). The increase in GPP was obvious in 2005, 2-year after clear-cutting, however GPP was still lower in 2010 at high temperature range compared with that before clear-cutting. Clear-cutting decreased RE at higher temperatures, and there was no apparent increasing trend of the reference respiration rate (R_{ref}) and apparent temperature sensitivity (E_a) throughout the following years (2003–2010) (Table 1).

The soil respiration rate during snow-free periods ranged between 8.52 and 11.05 Mg C ha^{-1} from 2003 to 2009, and its contribution to RE was 84 to 110%, although there was a large variance (SD = 28 to 44%) in the soil respiration rate among chambers (Table 3). The annual rate was estimated by adding the RE during the snow-covered period, which ranged between 8.92 and 11.61 Mg C ha^{-1} yr^{-1}. From 2003 to 2005, the soil respiration increased every year; however, there was no clear difference in the temperature sensitivities (E_a) from 2005 to 2009 (Fig. 3 and Table 1).

3.2. Biomass increments

The woody biomass of the mixed forest was 79.7±10.5 and 80.5±10.5 Mg C ha^{-1} in April 2002 and January 2003, respectively, and the annual carbon increment of the trees was therefore 0.75±0.05 Mg C ha^{-1} yr^{-1} during 2002. The planted larch, with an initial biomass of 0.04 Mg C ha^{-1}, increased at rates of 5.82±2.57 (mean±SD) mm yr^{-1} and 40.69±15.17 cm yr^{-1} for the basal diameter and the tree height, respectively, and as a result of this growth, the biomass increased to 1.04 ±0.02 Mg C ha^{-1} in 2009. Thus, the biomass increment was 1.00 ±0.02 Mg C ha^{-1} during the 7 years from 2003 to 2009.

462 *Sasa* biomass in the gaps (25.7±6.4 Mg C ha^{-1}) was more than double that in the understory
463 (11.9±2.0 Mg C ha^{-1}) before clear-cutting. The interannual PAI increment shows that PAI
464 doubled from 2003 to 2009 in rows where *Sasa* had not been strip-cut (Fig. 1), thus the biomass
465 increment in those rows during the 7 years was assumed to equal the difference in biomass
466 between the gap and understory locations (13.8±6.4 Mg C ha^{-1}) for the *Sasa* that was formerly in
467 the understory of the mixed forest, whereas no biomass change was assumed for *Sasa* that was
468 formerly growing in gaps in the mixed forest. On the other hand, in the strip-cut rows, *Sasa*
469 biomass decreased to 0 in 2003, but increased to reach almost the same PAI as that in the rows
470 that had not been strip-cut by 2009. Thus, we considered the biomass in the gaps (25.7 Mg C ha^{-1})
471 to represent the biomass increment from 2003 to 2009 in the strip-cut rows. Because the strip-
472 cut and uncut rows each covered half of the study area and the gap ratio was roughly half of the
473 study site in the mixed forest (Takagi et al., 2009), we considered the total biomass increment of
474 *Sasa* during the study period to be 16.3±4.8 Mg C ha^{-1}, which equals the area-weighted average
475 of the biomass increment obtained in the two types of row (i.e., [0.5×25.7] + [0.25×13.8] +
476 [0.25×0]).
477
478 *3.3. Carbon balance before and after clear-cutting*
479 We summarized the carbon budget of the mixed forest (Fig. 4), including the other carbon flows
480 estimated by Takagi et al. (2009). The total ecosystem respiration was divided almost evenly into
481 halves between the aboveground respiration (7.3 Mg C ha^{-1} yr^{-1}) and soil respiration (6.7 Mg C
482 ha^{-1} yr^{-1}). The net carbon absorption of 0.44±0.5 Mg C ha^{-1} yr^{-1} was close to the biomass
483 increment of the trees (0.75±0.05 Mg C ha^{-1} yr^{-1}). To close the gap between the two estimates of

484 the carbon budget, we assumed that the carbon loss from the understory *Sasa*, litter and the soil
485 totaled 0.31 Mg C ha^{-1} yr^{-1}.

486 Based on the net carbon sources on an annual basis during the 7 years from 2003 to 2009,
487 the net carbon emission after clear-cutting was 14.7± (1.3–3.5) Mg C ha^{-1} using values of 64.5±
488 (2.6–7) and 79.2± (2.6–7) Mg C ha^{-1} for GPP and RE, respectively, despite net biomass
489 increments of 1.00 ±0.02 and 16.3±4.8 Mg C ha^{-1} for the larch and *Sasa*, respectively.
490 Accordingly, average annual net carbon emission, GPP, RE, and net biomass increments of larch
491 and *Sasa* were 2.1 ± (0.2–0.5), 9.2 ± (0.4–1), 11.3 ± (0.4–1), 0.14 ±0.003 and 2.3 ± 0.7Mg C ha^{-1}
492 yr^{-1}, respectively, during the 7 years (Fig. 4).

493 The net carbon loss to the atmosphere was 14.7 Mg C ha^{-1} during the 7 years, while the
494 biomass increment of larch and *Sasa* was 17.3 Mg C ha^{-1} in total. This means that there had been
495 a carbon source of ca. 32 Mg C ha^{-1} or 4.57 Mg C ha^{-1} yr^{-1} to balance the budget, and we
496 attribute this carbon source to the decomposition of soil and litter carbon, including stumps,
497 branches, twigs, and leaves left on the ground after clear-cutting. This estimated source value (32
498 Mg C ha^{-1}) was 83% of the biomass residues from the branches, twigs, and leaves left on the
499 ground (38.5 Mg C ha^{-1}) or 58% of the biomass residues including the stumps (55.5 Mg C h a^{-1}).
500 The net carbon loss from these sources can be an order of magnitude greater than the carbon loss
501 from the soil, litter and understory vegetation prior to clear-cutting (0.31 Mg C ha^{-1} yr^{-1}). The
502 large difference in the net biomass increment between larch and *Sasa* implies that the
503 contribution of larch to GPP is very minor compared with that of *Sasa* during this early stage
504 after the clear-cutting.
505

506 *3.4. Comparison between observed and simulated carbon fluxes and stocks*

Simulated monthly RE tended to be overestimated in winter and underestimated in summer after clear-cutting, which leads to the overestimation of simulated NEE in winter (Fig. 5), the large y-intercept of the regression line between the observed and simulated RE (Fig. 6), and the scattered relationship between simulated and observed NEE (Fig. 6). However, the simulated carbon storage changes and total fluxes were in good agreement with the observation during the carbon source period (2003–2009), not only for those observed at the forest in 2002 (Table 4), although simulated soil respiration (R_s) was close to the lowest value within the standard deviation of the observed R_s. This simulation showed that litter C decomposition (35.6 Mg C ha^{-1}) became 65% of R_s, and more than total soil+litter C decrease (34.1 Mg C ha^{-1}, here carbon accumulation of 1.5 Mg C ha^{-1} in the soil) during the carbon source period. The simulated annual NEE became carbon sink at 8th (in 2010) year after clear-cutting (i.e. the carbon compensation point was 7 years) and showed similar carbon sink-source-sink trend with that of the observation throughout the conduct of forest activities.

The model predicted that this ecosystem will recover all the emitted CO_2 and carbon (CO_2+logs) within 6–7 (year 2015–2016) and 11–13 (year 2020–2022) years after the ecosystem compensation point in 2009, respectively (Fig. 7). Within 15 years (year 2024) after the compensation point, the total and vegetation carbon will be restored and litter carbon will decrease down to the state before the clear-cutting. On the other hand, the soil carbon will keep a constant value throughout that period, and the increase will be less than 1% of soil carbon stock (or 1.5 Mg C ha^{-1}) at its maximum in 2009, 6 years after the clear-cutting.

4. Discussion

4.1. The ecosystem carbon compensation point

The ecosystem carbon compensation point can be defined as the number of years after a disturbance when the ecosystem became a carbon sink (or carbon-neutral) again on an annual basis (Kowalski et al., 2004), and we estimated this value to be 7 years in our study (Table 5). Two recently published studies (Amiro et al., 2010; Grant et al., 2010) synthesized the measurements from a range of stands to evaluate the carbon budget for chronosequences of forests after disturbances. In both syntheses, all ecosystems showed net carbon losses after the clear-cut, but became carbon sinks again within 20 years, and most of them became carbon sinks by 10 years (Table 5). Most of the individual studies involved boreal forests, and three of the studies were conducted in the same forest in Saskatchewan, Canada (Howard et al., 2004; Amiro et al., 2006; Zha et al., 2009). The estimated carbon compensation point ranged from 7 to 13 years in the Saskatchewan's cases (Table 5). The transition into a carbon sink after 3 to 4 years in a managed plantation (Clark et al., 2004) was much earlier than in the rest of the studies. This comparison shows that our compensation point is the shortish case in the geographical temperature gradient tending to be shorter compensation point in warmer forest, while cited studies have varieties in the disturbance type [clearcut for Schulze et al. (1999), Law et al. (2001), Clark et al. (2004), Howard et al. (2004), Kolari et al. (2004), Freeden et al. (2007) and Zha et al. (2009): fire-burned for Goulden et al. (2011): and these combination for Amiro et al. (2006) and Humphreys et al. (2006)], treatment after the disturbance [plantation for Clark et al. (2004), Humphreys et al. (2006) and Freeden et al. (2007): natural regeneration for other studies with seed sown or scarification at some sites], and pre-disturbance condition [plantation for Clark et al. (2004): pristine or naturally regenerated forest for other studies].

551 Cumulative NEE is a vital parameter for evaluating the duration before an ecosystem fully
552 recovers the total CO_2 emitted into the atmosphere after a disturbance. The total payback period
553 for the emitted CO_2 can be estimated as the cumulative NEE during the period when the forest
554 was a net carbon source divided by the NEE before the disturbance. At our study site, it would
555 take up to 34 years to recover all the carbon emitted during the net source period (Table 6).
556 However, the CO_2 absorption rate of the mixed forest was obtained by just 1.5 years observation.
557 Biome-BGC modeling showed that the average NEE was 0.91 ± 0.43 Mg C ha^{-1} yr^{-1} during the
558 last 10 years before the clear-cutting (1993–2002). The payback period becomes 17 years if we
559 use this average value for the estimation. In addition, the studied forest was approximately 200-
560 year-old, and observed NEE was smaller than those obtained in other younger forests (~50 years
561 old) in Hokkaido, northern Japan, which ranged from 2.1 to 2.6 Mg C ha^{-1} yr^{-1} (Nakai et al.,
562 2003; Shibata et al., 2005; Hirata et al., 2007). Thus, if a value of 2.0 Mg C ha^{-1} yr^{-1} is applied to
563 calculate the payback period, the period could be as short as 8 years, and we used this to
564 represent the fastest possible payback period. The range (8–34 years) becomes 20–91 years if we
565 include the carbon loss as timber (25 Mg C ha^{-1}).

566 Chronosequence studies of stands with different ages can only provide annual NEE during a
567 specified period, and they usually leave wide gaps in the NEE values until the stand turns into a
568 sink again. Given this constraint, we only analyzed a few sites (Table 6). The NEE series within
569 the measurement period in the youngest stand would become the first few years of the
570 chronosequence. The NEE series of older sites within the chronosequence follow according to
571 their ages in ascending manner. To obtain a complete series of pre- and post-harvest NEE values
572 until NEE reaches the turning point between source and sink, we used linear interpolation to fill

573 in the gaps. We then computed the cumulative net emission as the sum of all annual NEE values
574 just after the disturbance and just before NEE became negative.

575 Grant et al. (2010) shows measured CO_2 fluxes in three post-clear-cut chronosequences in
576 British Columbia (BC), Saskatchewan, and Quebec in Canada, however only BC sites were
577 analyzed due to difficulty in deriving a cumulative NEE at the other two sites. BC sites were
578 regarded as those that regenerated after clear-cutting in 2000 (HDF00), 1988 (HDF88), and 1949
579 (DF49) and they reported a carbon compensation point of 10 to 20 years. Data from 2001 to
580 2007 in HDF00 were assumed to be the NEE for the initial 7 years of the chronosequence (1989
581 to 1995). NEE from 2002 to 2004 in HDF88 (just before NEE became negative in 2005) was
582 retained, leaving 1996 to 2001 blank. Year 2005 marks the 17th year of the chronosequence thus
583 their assumption of the conversion into sink at this period. Because they also assumed a shift
584 from source to sink in the 10th year, we calculated the cumulative NEE up to the 9th year. The
585 resulting total carbon emission during net source period was 44.0 Mg C ha^{-1} in the 10th year and
586 57.2 Mg C ha^{-1} in the 17th year, indicating carbon payback periods of 8 to 23 years and 10 to 29
587 years, respectively (Table 6).

588 We also estimated the carbon payback period from Zha et al. (2009) study conducted in one
589 of the three sites (Saskatchewan) from Grant et al. (2010). It involved four *Pinus banksiana*
590 stands representing four critical stages of stand development: harvested in 2002 (HJP02), 1994
591 (HJP94), and 1975 (HJP75), and a mature old forest (OJP) measured from 2004 to 2005, with
592 ages of 2, 10, 29, and 90 years in 2004, respectively. After gap-filling to replace the missing data
593 in the chronosequence, the cumulative NEE reached 7.0 Mg C ha^{-1}, therefore the total carbon
594 payback period ranged from 10 to 88 years. Howard et al. (2004) performed a biomass survey in
595 five jack pine stands (0, 5, 10, 29, and 79 years old) and the transition from source to sink was

596 estimated to occur at the 7th year. Only the average NEE for each stand was available, but
597 summing the net emissions until the stand became carbon-neutral by filling the gaps between the
598 observations gives a total carbon emission of 6.9 Mg C ha^{-1} and a payback period of 3 to 17
599 years.

600 Goulden et al. (2011) combined year-round eddy covariance measurements with biometry
601 and biomass harvests along a chronosequence of boreal forest stands in central Manitoba,
602 Canada. The stands were 1, 6, 15, 23, 40, ~74, and ~154 years old. NEE observations at the 6-
603 and 15-year-old stands indicated that the transition occurred at ages of 11 or 12 years. It appears
604 that it will take 11 to 92 years to repay all the emitted CO_2 in these stands (6.3 or 6.4 Mg C ha^{-1}).

605 Based on this comparative analysis, the duration of recovery to carbon neutrality after a
606 disturbance varies in response to differences in climate, ecosystem type, and the different
607 intensities and types of disturbance (Goulden et al., 2011). In most of these studies, the fastest
608 possible payback period was roughly equal to the time required to reach the carbon
609 compensation point, except for the study of Howard et al. (2004), which implies that the turning
610 point to become a carbon sink probably occurs midway through the payback period. However,
611 the longest estimated possible payback period shows that most of the sites may still take two or
612 more decades after once more becoming carbon sinks before they can recover all the emitted
613 CO_2.

614

615 *4.2 Uncertainties in the model simulation and observation*

616 The carbon cycle in the mixed forest was well simulated with minor adjustments on the
617 parameter sets proposed by Pietsch et al. (2005) for *Quercus robur/petraea*. After the clear-
618 cutting, we decreased parameter values on new fine root C to new leaf C allocation, new coarse

root C to new stem C allocation, and increased other parameters for allocation, fraction of leaf N in Rubisco, and maximum stomatal conductance to simulate the observed carbon fluxes and storages. Most of the revised parameter values are within the possible range reported by previous studies (White et al., 2000; Pietsch et al., 2005), however, the value (0.2) for new fine root C to new leaf C allocation was close to the minimum end of the possible range reported for wet grassland (0.199; Lewis Smith and Walton, 1975), wet meadow (0.338; Bliss, 1977), and mixed grass (0.281; Kumar and Joshi, 1972). Because *Sasa*, dwarf bamboo, behaves like a perennial grass or shrub and the clear-cutting increased the soil water content of the study site (Takagi et al., 2005b), it can be acceptable to use the similar parameter value with those for wet grassland ecosystems.

Additionally, high contribution of live wood C to total wood C (0.7) is rather close to the value for shrub (1.0) than the average for deciduous trees (0.16) (White et al., 2000), and does not contradict to the characteristic of *Sasa*, which emerges new culms every year from the soil, and the average culm age is < 5 years (Nishimura et al., 2004). Because of the difficulty in simulating the small and frequent disturbances during the plant growing period, we simulated the *Sasa* weeding during 2004–2006 by increasing the whole plant mortality fraction after clear-cutting. This treatment could be the main reason for the low sensitivity in the simulated GPP to the disturbance in 2004 and subsequent recovery during 2005–2007 (Fig.5).

Modeled monthly RE was overestimated in winter and underestimated in summer after clear-cutting (Figs 5 and 6), which is considered to be caused by low temperature sensitivity of the model. Another mismatch between the model and the observed was found in the soil respiration rate during the carbon source period. The observed annual soil respiration rate was

almost equal to RE for the 7 years, as mentioned by Takagi et al. (2009) for the first 3 years after clear-cutting. Although RE may have been systematically underestimated considering the energy balance ratio (0.74±0.03) obtained in our study site, they explained this large contribution of soil respiration by showing high root respiration rate of *Sasa* species and concluded that the respiration rate from the aboveground part was likely less than 20–30% of the observed soil respiration and within the large standard deviation (28–44%, 36% in average of 7 years) of the annual soil respiration rate among chambers. Decomposition of stumps, branches, twigs, and leaves left on the ground after clear-cutting of trees or strip-cutting of *Sasa* could have been considered as another reason for the high soil respiration rate. However, the modeled soil respiration rate during the 7 years after clear-cutting (2003–2009) was approx. 70% of the observed (Table 4), although the model also includes the effect of respiration from stumps and residuals after clear-cutting. This implies that the real soil respiration rate may be closer to the lower end of the large standard deviation in the observed.

The model predicted faster recovery of emitted CO_2 (6–7 years) than assumption from observed results (8–34 years), and forecasted that the vegetation carbon will be restored within 15 years (year 2024) after the compensation point (Fig. 7). However, considering the steep increase in the vegetation carbon content, the predicted recovery process might be overestimated, and our parameter set used for the clearcut may only be available during the early stage of the recovering period. If so, we may need further modification on the parameter set according with the tree growth and corresponding suppression of *Sasa* growth. This would be the limits when applying one-canopy layer model and must be confirmed by further continuous flux monitoring.

Involving these shortcomings, BIOME-BGC model simulated observed carbon flux and stock terms (Table 4), and showed similar carbon sink-source-sink trend with the observation throughout the forestry activities. This simulation showed that litter C decomposition (35.6 Mg C ha^{-1}) became 65% of R_s, and more than total soil+litter C decrease (34.1 Mg C ha^{-1}, here carbon accumulation of 1.5 Mg C ha^{-1} in the soil) during the carbon source period, and confirmed that litters including harvest residues were the major source of the emitted CO_2, as suggested by Noormets et al. (2012), and that the clear-cutting affected little on the soil carbon stock, as reported by Johnson (1992).

5. Conclusions

Clear-cutting caused large and long lasting CO_2 emission from the ecosystem and turned the litter including harvest residues into a large carbon emitter. The net carbon loss from the litter after the clear-cutting and before the carbon compensation point was an order of magnitude greater than that from soil+litter+undergrowth in the undisturbed forest on an annual basis. BIOME-BGC simulated the changes in the carbon fluxes and the stocks caused by the forest management in our study site, although further modification on the parameter set may be needed according with the tree growth and corresponding suppression of *Sasa* growth. This connotes that a quantitative prediction of the disturbance effect, which includes the ecosystem carbon compensation point and the total CO_2 emission during the carbon source period after the disturbance, can be made using a mechanistic model that is useful towards achieving a well-CO_2 managed forest thereby minimizing CO_2 increases in the atmosphere.

Acknowledgements

This research was a collaboration among Hokkaido University, National Institute for Environmental Studies, and Hokkaido Electric Power Co., Inc. through the project "CC-LaG Experiment," and it was partly supported by Grants-in-Aid for Scientific Research (no. 22310019) from MEXT, the A3 Foresight Program (CarboEastAsia) and Scientific Research on Innovation Areas (nos 20120012 and 21114008) of JSPS. We thank the staff of Teshio Experimental Forest for their support.

691 **References**

692 Aguilos, M., Takagi, K., Liang, N., Watanabe, Y., Teramoto, M., Goto, S., Takahashi, Y., Mukai,
693 H., Sasa, K., 2013. Sustained large stimulation of soil heterotrophic respiration rate and
694 its temperature sensitivity by soil warming in a cool-temperate forested peatland. Tellus
695 B, 65, 20792, http://dx.doi.org/10.3402/tellusb.v65i0.20792.
696 Amiro, B. D., Barr, A. G., Barr, J. G., Black, T. A., Bracho, R., Brown, M., Chen, J., Clark, K. L.,
697 Davis, K. J., Desai, A. R., Dore, S., Engel, V., Fuentes, J. D., Goldstein, A. H., Goulden,
698 M. L., Kolb, T. E., Lavigne, M. B., Law, B. E., Margolis, H. A., Martin, T., McCaughey,
699 J. H., Misson, L., Montes-Helu, M., Noormets, A., Randerson, J. T., Starr, G., Xiao, J.,.
700 2010. Ecosystem carbon dioxide fluxes after disturbance in forests of North America. J.
701 Geophys. Res. G: Biogeosci. 115, G00K02, doi: 10.10.1029/2010JG001390.
702 Amiro, B. D., Barr, A.G., Black, T. A., Iwashita, H., Kljun, N., McCaughey, J. H., Morgenstern,
703 K., Murayama, S., Nesic, Z., Orchansky, A. L., Saigusa, N., 2006. Carbon, energy and
704 water fluxes at mature and disturbed forest sites, Saskatchewan, Canada. Agric. For.
705 Meteorol. 136, 237–251.
706 Bliss, L. C., 1977. General summary Truelove Island ecosystem, in: Bliss, L. C. (Ed.), Truelove
707 Lowland, Devon Island, Canada: A High Arctic Ecosystem. University of Alberta Press,
708 Edmonton, Canada, pp. 657–675.
709 Bond-Lamberty, B., Wang, C., Gower. S. T., 2004. Net primary production and net ecosystem
710 production of a boreal black spruce wildfire chronosequence. Global Change Biol. 10,
711 473–487.
712 Clark, K. L., Gholz, H. L., Castro, M. S., 2004. Carbon dynamics along a chronosequence of
713 slash pine plantations in north Florida. Ecol. Appl. 14, 1154–1171.

714 Enting, I. G., Wigley, T. M. L., Heimann, M., 1994. Future emissions and concentrations of
715 carbon dioxide: key ocean/atmosphere/land analyses. CSIRO Division of Atmospheric
716 Research Technical Paper 31, 120pp.
717 Farquhar, G. D., Caemmerer, S. V., Berry, J. A., 1980. A biochemical model of photosynthetic
718 CO_2 assimilation in leaves of C_3 species. Planta 149, 79–90.
719 Falge, E., Baldocchi, D., Olson, R., Anthoni, P., Aubinet, M., Bernhofer, Ch., Burba, G.,
720 Ceulemans, R., Clement, R., Dolman, H., Granier, A., Gross, P., Grünwald, T., Hollinger,
721 D., Jensen, N. O., Katul, G., Keronen, P., Kowalski, A., Lai, C. T., Law, B. E., Meyers,
722 T., Moncrieff, J., Moors, E., Munger, J. W., Pilegaard, K., Rannik, Ü., Rebmann, C.,
723 Suyker, A., Tenhunen, J., Tu, K., Verma, S., Vesala, T., Wilson, K., Wofsy, S., 2001.
724 Gap filling strategies for defensible annual sums of net ecosystem exchange. Agric. For.
725 Meteorol. 107, 43–69.
726 Foken, T, Wichura, B., 1996. Tools for quality assessment of surface-based flux measurements.
727 Agric. For. Meteorol. 78, 83–105.
728 Freeden, A. L., Waughtal, J. D., Pypker, T. G., 2007. When do replanted sub-boreal clearcuts
729 become net sinks for CO_2? For. Ecol. Manage. 239, 210–216.
730 Giasson, M. –A., Coursolle, C., Margolis, H. A., 2006. Ecosystem-level CO_2 fluxes from a
731 boreal cutover in eastern Canada before and after scarification. Agric. For. Meteorol. 140,
732 23–40.
733 Goulden, M. L., McMillan, A. M. S., Winston, G. C., Rocha, A. V., Manies, K. L., Harden, J. W.,
734 Bond-Lamberty, B. P., 2011. Patterns of NPP, GPP, respiration, and NEP during boreal
735 forest succession. Global Change Biol.17, 855–871.

736 Grant, R. F., Barr, A. G., Black, T. A., Margolis, H. A., McCaughey, J. H., Trofymow, J. A.,
737 2010. Net ecosystem productivity of temperate and boreal forests after clearcutting: a
738 Fluxnet-Canada measurement and modeling synthesis. Tellus B 62(5), 475–496.
739 Hignett, P., 1992. Corrections to temperature measurements with a sonic anemometer.
740 Boundary-Layer Meteorol. 61, 175–187.
741 Hirata, R., Hirano, T., Saigusa, N., Fujinuma, Y., Inukai, K., Kitamori, Y., Takahashi, Y.,
742 Yamamoto, S., 2007. Seasonal and interannual variations in carbon dioxide exchange of a
743 temperate larch forest. Agric. For. Meteorol. 147, 110–124.
744 Hirata, R., Saigusa, N., Yamamoto, S., Ohtani, Y., Ide, R., Asanuma, J., Gamo, M., Hirano, T.,
745 Kondo, H., Kosugi, Y., Li, S. -G., Nakai, Y., Takagi, K., Tani, M., Wang, H., 2008.
746 Spatial distribution of carbon balance in forest ecosystems across East Asia. Agric. For.
747 Meteorol. 148, 761–775.
748 Houghton, R. A., 2003. Revised estimates of the annual net flux of carbon to the atmosphere
749 from changes in land use 1850–2000. Tellus B 55, 378–390.
750 Howard, E. A., Gower, S. T., Foley, J. A., Kucharik, C. J., 2004. Effects of logging on carbon
751 dynamics of a jack pine forest in Saskatchewan, Canada. Global Change Biol.10, 1267–
752 1284.
753 Humphreys, E.R., Black, T. A., Morgenstern, K., Cai, T., Drewitt, G. B., Nesic, Z., Trofymow, J.
754 A., 2006. Carbon dioxide fluxes in coastal Douglas-fir stands at different stages of
755 development after clearcut harvesting. Agric. For. Meteorol. 140, 6–22.
756 Jarvis, P. G., 1976. The interpretation of the variations in leaf water potential and stomatal
757 conductance found in canopies in the field. Philos. Trans. R. Soc. London, Ser. B 273,
758 593–610.

759 Johnson, D. W., 1992. Effects of forest management on soil carbon storage. Water Air Soil
760 Pollut. 64, 83–120.
761 Kaimal, J. C., Gaynor, J. E., 1991. Another look at sonic thermometry. Boundary-Layer
762 Meteorol. 56, 401–410.
763 Kimball, J. S., Thornton, P. E., White, M. A., Running, S. W., 1997a. Simulating forest
764 productivity and surface-atmosphere carbon exchange in the BOREAS study region. Tree
765 Physiol. 17, 589–599.
766 Kimball, J. S., White, M. A., Running, S. W., 1997b. BIOME-BGC simulations of stand
767 hydrologic processes for BOREAS. J. Geophys. Res. D: Atmos. 102, 29043–29051.
768 Koike, T., Hoyjo, H., Naniwa, A., Ashiya, D., Sugata, S., Sugishita, Y., Kobayashi, M., Nomura,
769 M., Akibayashi, Y., Nakajima, J., Takagi, K., Shibata, H., Satoh, F., Wang, W., Takada,
770 M., Fujinuma, Y., Shi, F., Matsuura, Y., Sasa, K., 2001. Basic data for CO_2 flux
771 monitoring of a young larch plantation: current status of a mature, mixed conifer-
772 broadleaf forest stand. Eurasian J. For. Res. 2, 65–79.
773 Kolari, P., Pumpanen, J., Rannik, Ü., Ilvesniemi, H., Hari, P., Berninger, F., 2004. Carbon
774 balance of different aged Scots pine forests in southern Finland. Global Change Biol. 10,
775 1106–1119.
776 Kormann, R., Meixner, F. X., 2001. An analytical footprint model for non-neutral stratification.
777 Boundary-Layer Meteorol. 99, 1106–1119.
778 Kowalski, A. S., Loustau, D., Berbigier, P., Manca, G., Tedeschi, V., Borghetti, M., Valentini, R.,
779 Kolari, P., Berninger, F., Rannik, Ü., Hari, P., Rayment, M., Mencuccini, M., Moncrieff,
780 J., Grace, J., 2004. Paired comparisons of carbon exchange between undisturbed and

781 regenerating stands in four managed forests in Europe. Global Change Biol. 10, 1707–
782 1723.
783 Kowalski, S., Sartore, M., Burlett, R., Berbigier, P., Loustau, D., 2003. The annual carbon
784 budget of a French pine forest (*Pinus pinaster*) following harvest. Global Change Biol. 9,
785 1051–1065.
786 Kumar, A., Joshi, M. C., 1972. The effect of grazing on the structure and productivity of
787 vegetation near Pilani, Rajasthan, India. J. Ecol. 60, 665–675.
788 Law, B.E., Thornton, P. E., Irvine, J., Anthoni, P. M., Van Tuyl, S., 2001. Carbon storage and
789 fluxes in ponderosa pine forests at different developmental stages. Global Change Biol. 7,
790 755–777.
791 Leuning, R., King, K. M., 1992. Comparison of eddy-covariance measurements of CO_2 fluxes by
792 open- and closed-path CO_2 analysers. Boundary-Layer Meteorol. 59, 297–311.
793 Lewis Smith, R. I., Walton, D. W. H., 1975. South Georgia, Subantarctic, in: Rosswall, T., Heal,
794 O. W. (Eds.), Structure and Function of Tundra Ecosystems. Swedish Natural Science
795 Research Council, Stockholm, Sweden, pp. 399–423.
796 Liang, N., Hirano, T., Zheng, Z. M., Tang, J., Fujinuma, Y., 2010. Soil CO_2 efflux of a larch
797 forest in northern Japan. Biogeosciences 7, 3447−3457.
798 Lloyd, J., Taylor, J. A., 1994. On the temperature dependence of soil respiration. Funct. Ecol. 8,
799 315–323.
800 Mano, M., Miyata, A., Yasuda, Y., Nagai, H., Yamada, T., Ono, K., Saito, M., Kobayashi, Y.,
801 2007. Quality control for the open-path eddy covariance data. J. Agric. Meteorol. 63,
802 125–138 (in Japanese with English abstract and figure captions).

803 Mission, L., Tang, J., Xu, M., McKay, M., Goldstein, A. H., 2005. Influences of recovery from
804 clear-cut, climate variability, and thinning on the carbon balance of a young ponderosa
805 pine plantation. Agric. For. Meteorol. 149, 783–794.
806 Moncrieff, J., Clement, R., Finnigan, J., Meyers, T., 2004. Averaging, detrending, and filtering
807 of eddy covariance time series, in: Lee, X., Massman, W., Law, B. (Eds), Handbook of
808 Micrometeorology: A guide for surface flux measurement and analysis. Kluwer
809 Academic Publishers, Dordrecht, the Netherlands, pp. 7–31.
810 Moore, C. J., 1986. Frequency response corrections for eddy correlation systems. Boundary-
811 Layer Meteorol. 37, 17–35.
812 Nakai, Y., Kitamura, K., Suzuki, S., Abe, E., 2003. Year-long carbon dioxide exchange above
813 broadleaf deciduous forest in Sapporo, northern Japan. Tellus B 55, 305–312.
814 Nishimura, N., Matsui, Y., Ueyama, T., Mo, W., Saijo, S., Tsuda, S., Yamamoto, S., Koizumi,
815 H., 2004. Evaluation of carbon budgets of a forest floor *Sasa senanensis* community in a
816 cool-temperate forest ecosystem, central Japan. Japanese J. Ecol. 54, 143–158 (in
817 Japanese with English abstract and figure captions).
818 Noormets, A., McNulty, S. G., Domec, J. -C., Gavazzi, M., Sun, G., King, J. S., 2012. The role
819 of harvest residue in rotation cycle carbon balance in loblolly pine plantations.
820 Respiration partitioning approach. Global Change Biol.18, 3186–3201.
821 Pietsch, S. A., Hasenauer, H., Thornton, P. E., 2005. BGC-model parameters for tree species
822 growing in central European forests. For. Ecol. Manage. 211, 264–295.
823 Pongratz, J., Reick, C. H., Raddatz, T., Claussen, M., 2009. Effects of anthropogenic land cover
824 change on the carbon cycle of the last millennium. Global Biogeochem. Cycles 23,
825 GB4001, doi:10.1029/2009GB003488.

826 Reichstein, M., Falge, E., Baldocchi, D., Papale, D., Aubinet, M., Berbigier, P., Bernhofer, Ch.,
827 Buchmann, N., Gilmanov, T., Granier, A., Grünwald, T., Havránková, K., Ilvesniemi, H.,
828 Janous, D., Knohl, A., Laurila, T., Lohila, A., Loustau, D., Matteucci, G., Meyers, T.,
829 Miglietta, F., Ourcival, J. -M., Pumpanen, J., Rambal, S., Rotenberg, E., Sanz, M.,
830 Tenhunen, J., Seufert, G., Vaccari, F., Vesala, T., Yakir, D., Valentini, R., 2005. On the
831 separation of net ecosystem exchange into assimilation and ecosystem respiration: review
832 and improved algorithm. Global Change Biol.11, 1424–1439.
833 Schulze, E.-D., Lloyd, J., Kelliher, F. M., Wirh, C., Rebmann, C., Lühker, B., Mund, M., Knohl,
834 A., Milyukova, I. M., Schulze, W., Ziegler, W., Varlagin, A. B., Sogachev, A. F.,
835 Valentini, R., Dore, S., Grigoriev, S., Kolle, O., Panfyorov, M. I., Tchebakova, N.,
836 Vygodskaya, N. N., 1999. Productivity of forests in the Eurosiberian boreal region and
837 their potential to act as carbon sink: a synthesis. Global Change Biol.5, 703–722.
838 Shibata, H., Hiura, T., Tanaka, Y., Takagi, K., Koike, T., 2005. Carbon cycling and budget in a
839 forested basin of southwestern Hokkaido, northern Japan. Ecol. Res. 20, 325–331.
840 Takagi, K., 2012. Latent heat flux estimation using closed-path and low-frequency water vapor
841 concentration sensors. J. Agric. Meteorol. Hokkaido, 64, 4–12 (in Japanese).
842 Takagi, K, Fukuzawa, K., Liang, N., Kayama, M., Nomura, M., Hojyo, H., Sugata, S., Shibata,
843 H., Fukazawa, T., Takahashi, Y., Nakaji, T., Oguma, H., Mano, M., Akibayashi, Y.,
844 Murayama, T., Koike, T., Sasa, K., Fujinuma, Y., 2009. Change in CO_2 balance under a
845 series of forestry activities in a cool-temperate mixed forest with dense undergrowth.
846 Global Change Biol. 15(5), 1275–1288.
847 Takagi, K., Kotsuka, C., Fukuzawa, K., Kayama, M., Makoto, K., Watanabe, T., Nomura, M.,
848 Fukazawa, T., Takahashi, H., Hojyo, H., Ashiya, D., Naniwa, A., Sugata, S., Kamiura, T.,

Sugishita, Y., Sakai, R., Ito, K., Kobayashi, M., Maebayashi, M., Mizuno, M., Murayama, T., Kinoshita, K., Fujiwara, D., Hashida, S., Shibata, H., Yoshida, T., Sasa, K., Saigusa, N., Fujinuma, Y., Akibayashi, Y., 2010. Allometric relationships and carbon and nitrogen contents for three major tree species (*Quercus crispula*, *Betula ermanii*, and *Abies sachalinensis*) in northern Hokkaido, Japan. Eurasian J. For. Res. 13(1), 1–7.

Takagi, K., Nomura, M., Ashiya, D., Takahashi, H., Sasa, K., Fujinuma, Y., Shibata, H., Akibayashi, Y., Koike, T., 2005a. Dynamic carbon dioxide exchange through snowpack by wind-driven mass transfer in a conifer-broadleaf mixed forest in northernmost Japan. Global Biogeochem. Cycles 19, GB2012, doi:10.1029/2004GB002272.

Takagi, K., Nomura, M., Fukuzawa, K., Kayama, M., Shibata, H., Sasa, K., Koike, T., Akibayashi, Y., Fujinuma, Y., Inukai, K., Maebayashi, M., 2005b. Deforestation effects on the micrometeorology in a cool-temperate forest in northernmost Japan. J. Agric. Meteorol. 60, 1025–1028.

Takahashi, H., Takagi, K., Nomura, M., Hojyo, H., Kamiura, T., Kozuka, C., Sakai, R., Yone, Y., Fukushi, R., Oguma, H., Fujinuma, Y., Maebayashi, M., 2006. Tree height and biomass evaluation at conifer-hardwood mixed forest in northern Hokkaido using airborne Laser survey. Trans. Mtg. Hokkaido Br. Jpn. For. Soc. 54, 93–95 (in Japanese).

Tans, P. P., Conway, T. J., 2005. Monthly atmospheric CO_2 mixing ratios from the NOAA CMDL carbon cycle cooperative global air sampling network, 1968–2002. In Trends: A compendium of data on global change. Carbon dioxide information analysis center, Oak Ridge National Laboratory, U. S. Department of Energy, Oak Ridge, Tennessee, U.S.A.

Taylor, J. R., 1997. Propagation of uncertainties, in: Taylor, J. R. (Ed.), An introduction to error analysis 2nd ed, University Science Books, Sausalito, CA, USA, pp. 45–91.

872 Thornton, P. E., Law, B. E., Gholz, H. L., Clark, K. L., Falge, E., Ellsworth, D. S., Goldstein, A.
873 H., Monson, R. K., Hollinger, D., Falk, M., Chen, J., Sparks, J. P., 2002. Modeling and
874 measuring the effects of disturbance history and climate on carbon and water budgets in
875 evergreen needleleaf forests. Agric. For. Meteorol. 113, 185–222.
876 Tsuji, H., Nakatsuka, T., Takagi, K., 2006. $\delta^{18}O$ of tree-ring cellulose in two species (spruce and
877 oak) as proxies of precipitation amount and relative humidity in northern Japan. Chem.
878 Geol. 231, 67-76.
879 Ueyama, M., Harazono, Y., Kim, Y., Tanaka, N., 2009. Response of the carbon cycle in sub-
880 arctic black spruce forests to climate change: Reduction of a carbon sink related to the
881 sensitivity of heterotrophic respiration. Agric. For. Meteorol. 149, 582–602.
882 Vickers, D., Mahrt, L., 1997. Quality control and flux sampling problems for tower and aircraft
883 data. J. Atmos. Ocean. Technol. 14, 512–526.
884 Walker, L. R., Wardle, D. A., Bardgett, R. D., Clarkson, B. D., 2010. The use of
885 chronosequences in studies of ecological succession and soil development. J. Ecol. 98,
886 725–736.
887 White, M. A., Thornton, P. E., Running, S. W., Nemani, R. R., 2000. Parameterization and
888 sensitivity analysis of the BIOME-BGC terrestrial ecosystem model: Net primary
889 production controls. Earth Interact. 4, 1–85.
890 Wilczak, J.M., Oncley, S. P., Stage, S. A., 2001. Sonic anemometer tilt correction algorithms.
891 Boundary-Layer Meteorol. 99, 127–150.
892 Wilson, K., Goldstein, A., Falge, E., Aubinet, M., Baldocchi, D., Berbigier, P., Bernhofer, C.,
893 Ceulemans, R., Dolman, H., Field, C., Grelle, A., Ibrom, A., Law, B. E., Kowalski, A.,
894 Meyers, T., Moncrieff, J., Monson, R., Oechel, W., Tenhunen, J., Valentini, R., Verma,

S., 2002. Energy balance closure at FLUXNET sites. Agric. For. Meteorol., 113, 223–243.

Zha, T., Barr, A. G., Black, T. A., McCaughey, J. H., Bhatti, J., Hawthorne, I., Krishnan, P., Kidston, J., Saigusa, N., Shashkov, A., Nesic, Z., 2009. Carbon sequestration in boreal jack pine stands following harvesting. Global Change Biol. 15, 1475–1487.

Table 1 Interannual variation in the respiratory parameters (values are means followed by the SD in parentheses) for ecosystem respiration (RE) and soil respiration (R_s). R_{ref} is the respiration rate (μmol m^{-2} s^{-1}) at the reference temperature (T_{ref} =283.15 *K*). E_a is the apparent temperature sensitivity (KJ mol^{-1}) .

		2002*	2003*	2004*	2005*	2006	2007	2008	2009	2010	2011
RE	R_{ref}	4.22 (0.31)	3.07 (0.21)	3.28 (0.30)	3.20 (0.14)	2.91 (0.14)	3.53 (0.20)	3.48 (0.14)	2.97 (0.31)	3.33 (0.27)	2.60 (0.21)
	E_a	63.43 (5.07)	70.40 (5.48)	35.44 (6.02)	66.54 (3.11)	75.40 (3.25)	68.57 (3.92)	56.33 (2.84)	61.81 (7.30)	50.25 (4.40)	76.01 (4.73)
R_s	R_{ref}	–	3.35 (0.18)	3.70 (0.09)	3.85 (0.11)	3.47 (0.15)	3.99 (0.20)	3.66 (0.15)	3.73 (0.06)	–	–
	E_a	–	40.71 (5.75)	52.48 (2.43)	72.22 (2.98)	71.48 (3.99)	69.99 (4.53)	74.32 (4.67)	80.54 (2.16)	–	–

* The values from 2002 to 2005 are from Takagi et al. (2009).

908 **Table 2** Parameters used for the BIOME-BGC model.

Parameter (C=carbon, N=nitrogen)	Original[*1]	Improved for spinup run and simulation until 2002	Improved for simulation during 2003 to 2011
Yearday to start new growth (DOY)	–	80	110
Yearday to end litterfall (DOY)	–	310	310
Transfer growth period as fraction of growing season	0.25	0.3	0.15
Litterfall as fraction of growing season	0.3	0.3	0.15
Annual leaf and fine root turnover fraction (yr^{-1})	1.0	1.0	0.85
Annual live wood turnover fraction (yr^{-1})	0.7	0.7	0.85
Annual whole-plant mortality fraction (yr^{-1})	0.005	0.01	0.03
Annual fire mortality fraction (yr^{-1})	0.0	0.005	0.0
New fine root C : new leaf C (ratio)	1.2	1.6	0.2
New stem C : new leaf C (ratio)	1.32	1.0	2.0
New live wood C : new total wood C (ratio)	0.16	0.2	0.7
New coarse root C : new stem C (ratio)	0.26	0.26	0.1
Current growth proportion (ratio)	0.5	0.5	0.5
C:N of leaves/ falling leaf litter/ fine roots/ live wood/ dead wood (kg C kg N^{-1})	27.2/ 64.1/ 73.5/ 73.5/ 451	27.2/ 64.1/ 73.5/ 73.5/ 451	27.2/ 64.1/ 73.5/ 73.5/ 451
Leaf litter labile/ cellulose/ lignin proportion	0.20/ 0.56/ 0.24	0.20/ 0.56/ 0.24	0.20/ 0.56/ 0.24
Fine root labile/ cellulose/ lignin proportion	0.34/ 0.44/ 0.22	0.34/ 0.44/ 0.22	0.20/ 0.56/ 0.24
Dead wood cellulose/ lignin proportion	0.75/0.25	0.75/0.25	0.75/0.25
Canopy water interception coefficient (LAI^{-1} d^{-1})	0.038	0.038	0.038
Canopy light extinction coefficient	0.54	0.54	0.40
All-sided to projected leaf area ratio	2.0	2.0	2.0
Canopy average specific leaf area (m^2 kg C^{-1})	34.5	38.5	40.0
Ratio of shaded SLA:sunlit SLA*[2]	2.0	2.0	2.0
Fraction of leaf N in Rubisco	0.088	0.065	0.14
Maximum stomatal conductance (m s^{-1})	0.0024	0.0024	0.006
Cuticular conductance (m s^{-1})	0.00006	0.00006	0.00006
Boundary layer conductance (m s^{-1})	0.005	0.005	0.010
PSI[*3]: start of conductance reduction (MPa)	–0.5	–0.5	–0.5
PSI[*3]: complete conductance reduction (MPa)	–3.5	–3.5	–3.5
VPD[*4]: start of conductance reduction (kPa)	0.2	0.6	1.5
VPD[*4]: complete conductance reduction (kPa)	2.55	3.0	3.0

909 [*1] values for *Quercus robur/petraea* forest in Pietsch et al (2005); [*2] Specific leaf area; [*3] Leaf and soil water

910 potential; [*4] Vapor pressure deficit

911 **Table 3** Interannual variation in net ecosystem CO_2 exchange (NEE), gross primary production
912 (GPP), ecosystem respiration (RE), RE in the snow-free period (RE_g), soil respiration (R_s), and
913 R_s in the snow-free period (R_s_g). NEE, GPP, RE, and R_s are annual sums (Mg C ha^{-1} yr^{-1}), and
914 RE_g and R_s_g are the sums for the snow-free period (Mg C ha^{-1} per period). Values are means,
915 with SD in parentheses for the seasonal sum. R_s was evaluated by summing RE during the snow-
916 covered period and R_s_g.

917

	2002*	2003*	2004*	2005*	2006	2007	2008	2009	2010	2011
NEE	–0.44	5.69	4.95	1.53	1.17	0.04	1.03	0.28	–0.49	–0.52
GPP	14.39	4.81	5.40	10.14	10.28	12.25	11.16	10.35	12.38	11.66
RE	13.95	10.50	10.35	11.67	11.45	12.29	12.19	10.63	11.89	11.14
RE_g	13.01	10.10	9.51	10.96	10.63	11.73	11.21	9.48	11.07	10.53
R_s_g	–	8.52 (2.89)	10.47 (2.93)	10.62 (3.39)	9.81 (3.91)	11.05 (4.85)	10.35 (3.84)	9.48 (3.67)	–	–
R_s	–	8.92	11.31	11.33	10.64	11.61	11.34	10.63	–	–

918

919 *Values from 2002 to 2005 are from Takagi et al. (2009).

920

921 **Table 4** Comparison between observed and modeled carbon stocks and fluxes.

922

Carbon stocks and fluxes	Observation	Model
In 2002		
Vegetation carbon (Mg C ha^{-1})	99± 10.5[*1]	116
Soil carbon (Mg C ha^{-1})	159[*2]	165
Annual maximum projected LAI (m^2 m^{-2})	7.3[*3]	7.3
NEE (Mg C ha^{-1} yr^{-1})	–0.4± 0.5	–1.0
GPP (Mg C ha^{-1} yr^{-1})	14.4± 1	14.4
RE (Mg C ha^{-1} yr^{-1})	14.0± 1	13.3
During 2003–2009		
Soil+litter carbon decrease (Mg C ha^{-1})	~32	34.1
Vegetation carbon increase (Mg C ha^{-1})	17.2± 5	16.5
Cumulative NEE (Mg C ha^{-1})	14.7± 3.5	17.6
Cumulative GPP (Mg C ha^{-1})	64.5± 7	60.2
Cumulative RE (Mg C ha^{-1})	79.2± 7	77.8
Cumulative R_s (Mg C ha^{-1})	75.8± 22.3	54.8
Carbon compensation point (yr)	7	7

923

924 [*1] sum of trees and dwarf bamboos; [*2] up to 1m depth; [*3] sum of PAI of trees and dwarf bamboos

925 **Table 5** Carbon compensation points from different chronosequence studies across a range of
926 forest ecosystems.

Study site	Forest type	Dominant species	Stand ages along the chronosequence	Carbon compensation point (stand age)	Source
Synthesis studies					
B.C., Canada	Boreal forest	*Pseudotsuga menziesii*	7, 19, 58	10–20	Grant et al. (2010)
Saskatchewan, Canada	Boreal forest	*Pinus banksiana*	2, 10, 29, 90	10–20	
Quebec, Canada	Boreal forest	*Picea mariana*	3, 109	10–20	
North America	Various North			10–20	Amiro et al. (2010)
Saskatchewan	American forests	*P. banksiana*	2, 10, 29, 90		
Quebec		*P. mariana*	5, 33, 93		
Vancouver Island		*P. menziesii*	8, 20, 59		
New Brunswick		*Abies balsamea*	3, 4		
Wisconsin		*Hardwoods, and Pinus resinosa*	3, 6, 7, 11, 21, 58, 64, 73, 83		
Oregon		*Pinus ponderosa*	21, 24, 96		
Florida		*Pinus elliottii*,	9, 15, 35		
Arizona		*P. ponderosa*	2		
California		*P. ponderosa*	2, 12		
Individual studies					
Saskatchewan, Canada	Boreal upland forest	*P. banksiana*	0, 5, 10, 29, 79	~7	Howard et al. (2004)
Saskatchewan, Canada	Boreal upland forest	*P. banksiana*	4, 8, 13, 73	13	Amiro et al. (2006)
Saskatchewan, Canada	Boreal upland forest	*P. banksiana*	2, 10, 29, 90	10	Zha et al. (2009)
British Columbia, Canada	Second-growth boreal forest	*P. menziesii* var. *menziesii*	2, 14, 53	20	Humphreys et al. (2006)
British Columbia, Canada	Sub-boreal forest	*Picea glauca* × *engelmannii*	5, 6, 8, 10	8–10	Freeden et al. (2007)
Central Manitoba, Canada	Boreal forest	*P. mariana*	1, 6, 15, 23, 40, 74, 154	11–12	Goulden et al. (2011)
Southern Finland	Boreal forest	*Pinus sylvestris*	4, 12, 40, 75	12	Kolari et al. (2004)
Central Oregon, USA	Cool-temperate forest	*P. ponderosa*	21, 50, 250	10–20	Law et al. (2001)
Florida, USA	Warm-temperate forest	*P. elliottii* var. *elliottii*	0, 10, 24	3–4	Clark et al. (2004)
Siberia, Russia	Boreal forest	*P. sylvestris*	7, 13, 67, 200, 215	14	Schulze et al. (1999)
Hokkaido, northern Japan	Cool-temperate mixed forest	*Quercus crispula, Betula ermanii, Abies sachalinensis, Betula platyphylla* var. *japonica*, and *Picea jezoensis*	–	7	Present study

927 **Table 6** Estimated total CO_2 emission rate during the net source period and the payback period
928 for the ecosystem to recover the CO_2 emitted after the disturbance which will commence once
929 the ecosystem reach the carbon compensation point.

930

Study site	NEE prior to disturbance (Mg C ha^{-1} yr^{-1})	Cumulative NEE after the disturbance (Mg C ha^{-1})	Estimated number of years to recover the CO_2 emitted after the disturbance	Source
British Columbia, Canada EC-derived*				Grant et al. (2010)
ECP* at 10 years	–1.95 to –5.52	44.0	8–23	
ECP at 17 years		57.2	10–29	
Saskatchewan, Canada	–0.08 to –0.68	7.0	10–88	Zha et al. (2009)
Saskatchewan, Canada	–0.4 to –2.7	6.9	3–17	Howard et al. (2004)
Central Manitoba, Canada	–0.07 to –0.58	6.3–6.4	11–92	Goulden et al. (2011)
Hokkaido, northern Japan	–0.44 to ~ –2.0	14.7	8–34	Present study

931

932 * EC, eddy covariance method; ECP, ecosystem carbon compensation point.

933

934 **Figure captions**

935

936 **Fig. 1** Interannual variation of the plant area index (PAI). PAI includes the shade by the stems,
937 branches, and culms in addition to the leaves of the canopy. Clear-cutting occurred from
938 January to March 2003 (first dashed enclosure) and strip-cutting of *Sasa* to allow planting
939 of hybrid larch occurred in late October 2003 (second dashed enclosure). Gray shading
940 represents snow-covered periods. The PAI of each component was measured three to five
941 times every 2 to 4 weeks during the growing period; symbols represent the means; and
942 vertical bars denote max/min values. Two reference values (no canopy shade) and 10
943 sample values (with canopy shade) were measured to obtain each PAI value.

944

945 **Fig. 2** (*top*) Interannual variation of gross primary production (GPP), ecosystem respiration (RE),
946 and net ecosystem CO_2 exchange (NEE). Thick and narrow arrows represent periods of
947 clear-cutting and strip-cutting of *Sasa* and larch planting, respectively. (*bottom*) Cumulative
948 net ecosystem CO_2 exchange (NEE) from 2003 to 2011 and cumulative uncertainties during
949 the net source period (2003 to 2009). See Materials and Methods section for the estimation
950 of uncertainties.

951

952 **Fig. 3** Relation of (a) daily gross primary production (GPP) and (b) daily ecosystem respiration
953 (RE) to daily mean air temperature during the snow-free periods from 2002 to 2010, and (c)
954 relationship between the soil temperature at a depth of 5 cm and soil respiration rate during
955 snow-free periods from 2003 to 2009. Daily GPP and RE were classified into 2°C air

956 temperature classes and soil respiration was classified into 1°C soil temperature classes.
957 Symbols represent the means for each temperature class and vertical bars indicate ±1SD.
958 Table 1 summarizes the parameter values for RE and soil respiration obtained from the
959 regressions.
960
961 **Fig. 4** Carbon balance (a) in the mixed forest before clear-cutting in 2002, and (b) after clear-
962 cutting (from 2003 to 2009). Values in (b) are shown as mean annual rates for comparison.
963 Gray numbers represent the residuals required to balance the carbon budget. See text for
964 each estimation.
965
966 **Fig. 5** Decadal variation of modeled and observed monthly carbon fluxes.
967
968 **Fig. 6** Comparison between modeled and observed monthly carbon fluxes. Carbon fluxes before
969 (in 2002) and after (from 2003 to 2011) clear-cutting are shown by closed and open circles,
970 respectively. Linear regression equations are obtained by using all monthly data obtained
971 from 2002 to 2011.
972
973 **Fig. 7** Simulated carbon contents and fluxes from 2001 to 2025. Total, vegetation, litter, and soil
974 carbon contents and GPP, RE, NEE, and soil heterotrophic respiration (R_h) are shown.
975 Results from 2012 are obtained using the same parameter set with that used during 2003 to
976 2011 in Table 2 and are shown as the average and the standard deviation (vertical bars) of
977 10 simulation runs each of which used the repeated annual variation of micrometeorology

978 observed each year of the 10-year study period from 2002 to 2011 throughout the
979 simulation, although the errors for the carbon contents was too small to identify.
980

981 **Fig. 1**

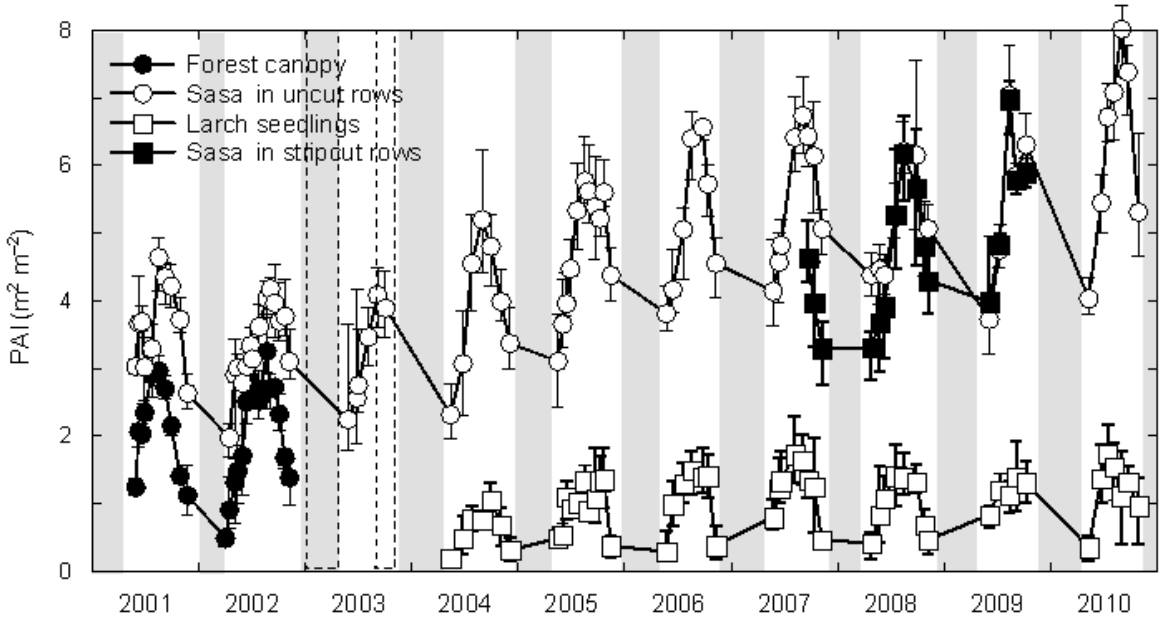

982

983

984 **Fig. 2**

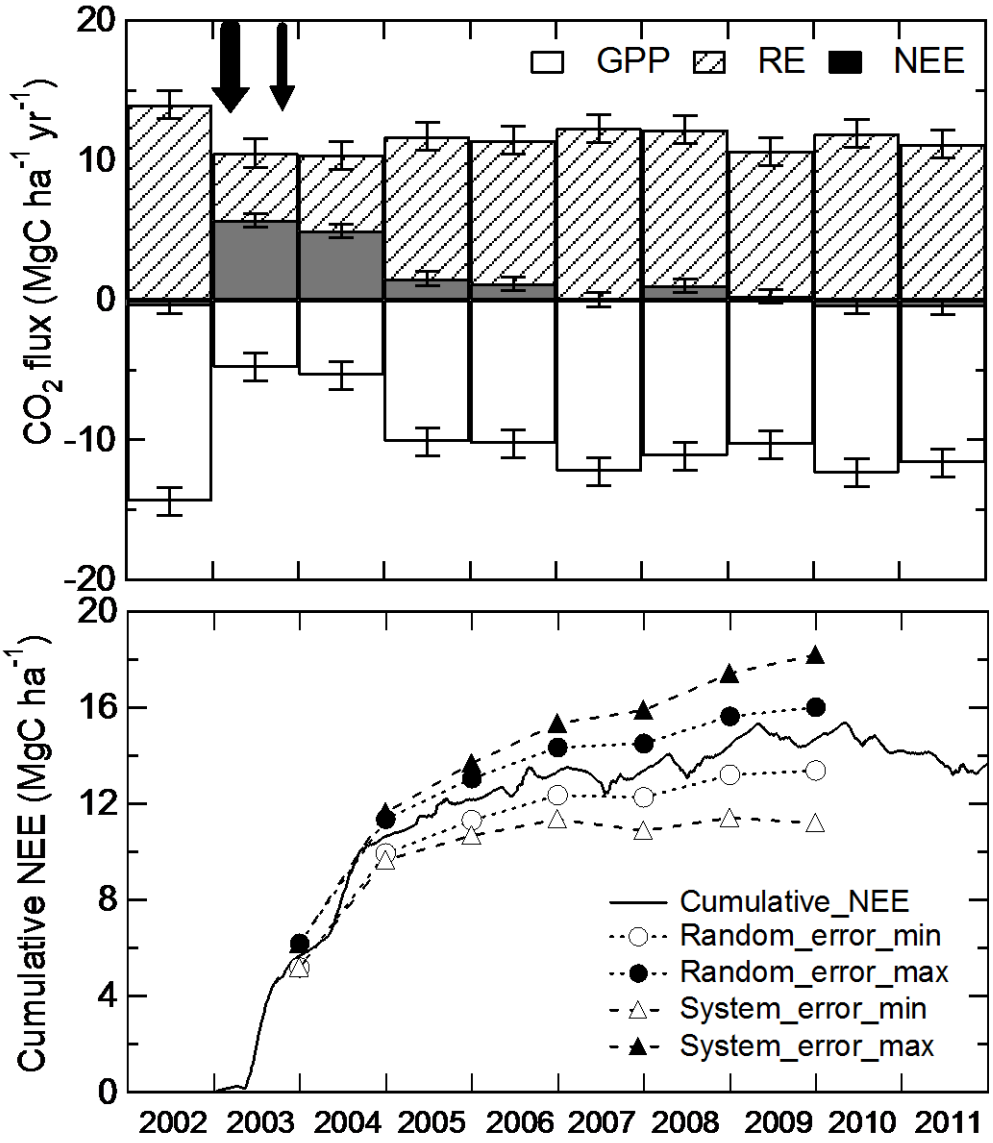

985

986

987

988 **Fig. 3**

989

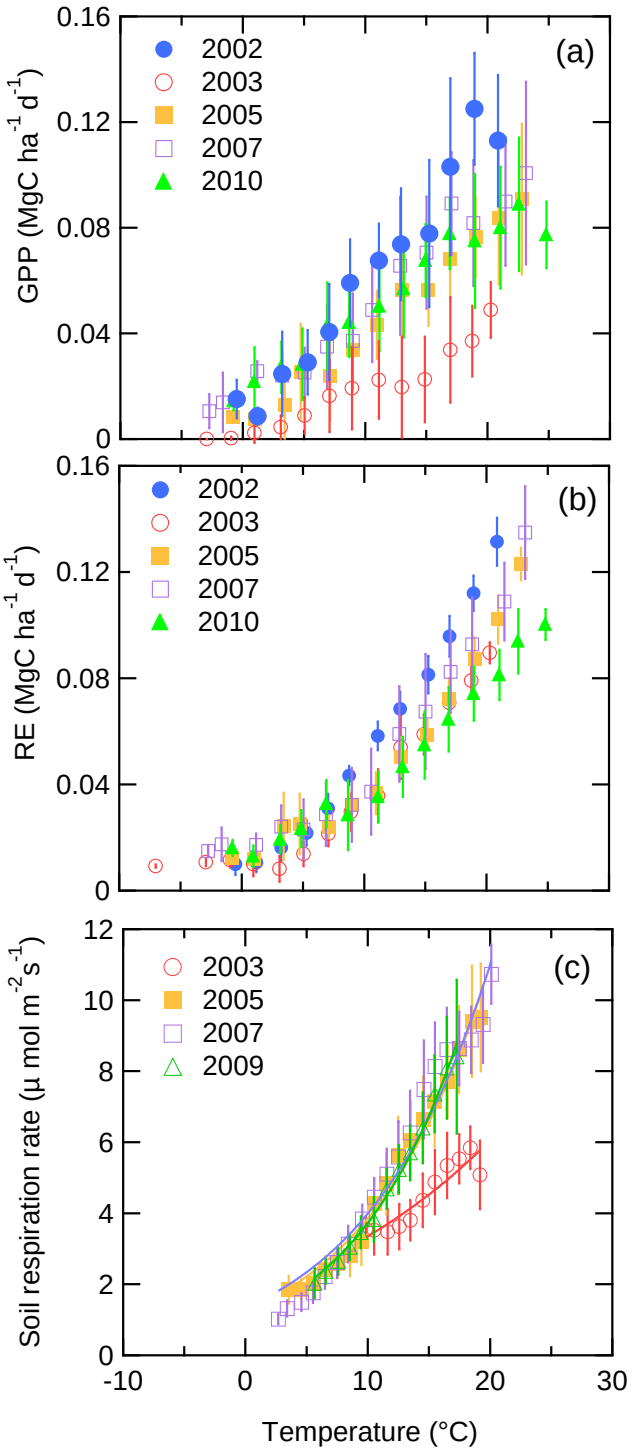
(a)
2002
2003
2005
2007
2010
GPP (MgC ha-1 d-1)
0.16
0.12
0.08
0.04
0
(b)
2002
2003
2005
2007
2010
RE (MgC ha-1 d-1)
0.16
0.12
0.08
0.04
0
(c)
2003
2005
2007
2009
Soil respiration rate (μ mol m-2 s-1)
12
10
8
6
4
2
0
-10
0
10
20
30
Temperature (°C)

990 **Fig. 4**

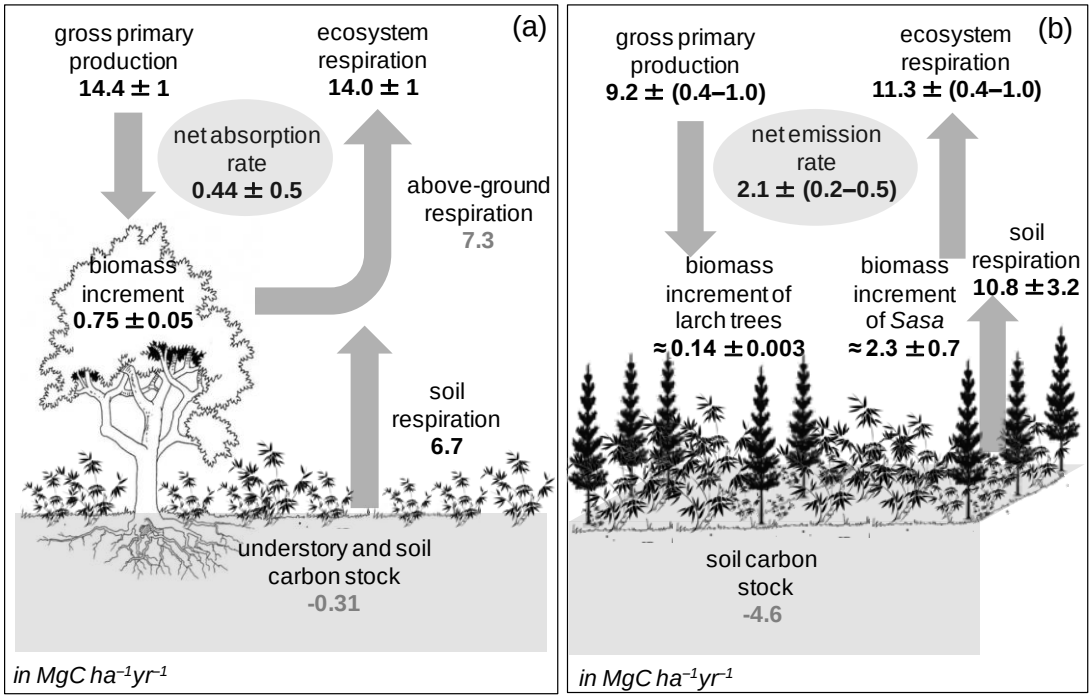

991

992

993 **Fig. 5**

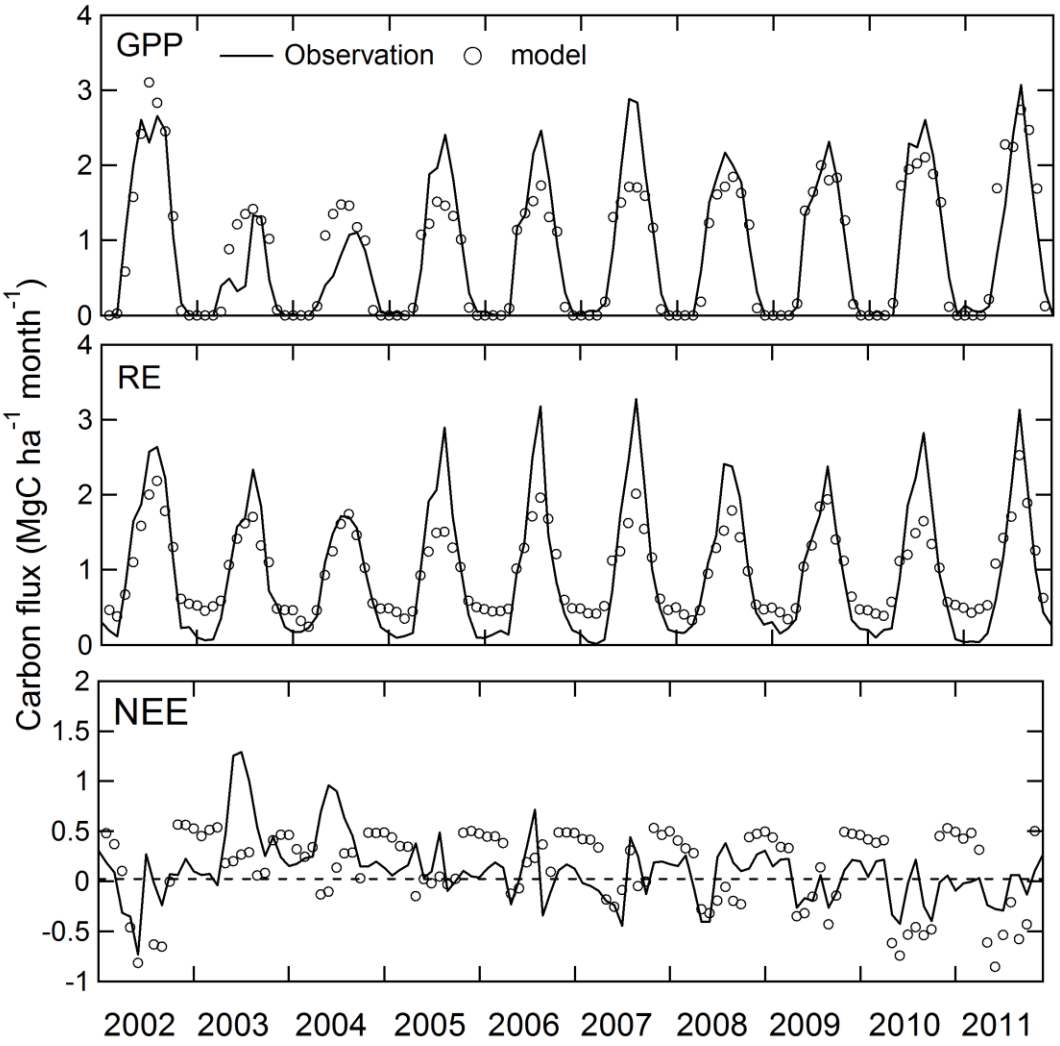

994

995

996 **Fig. 6**

997

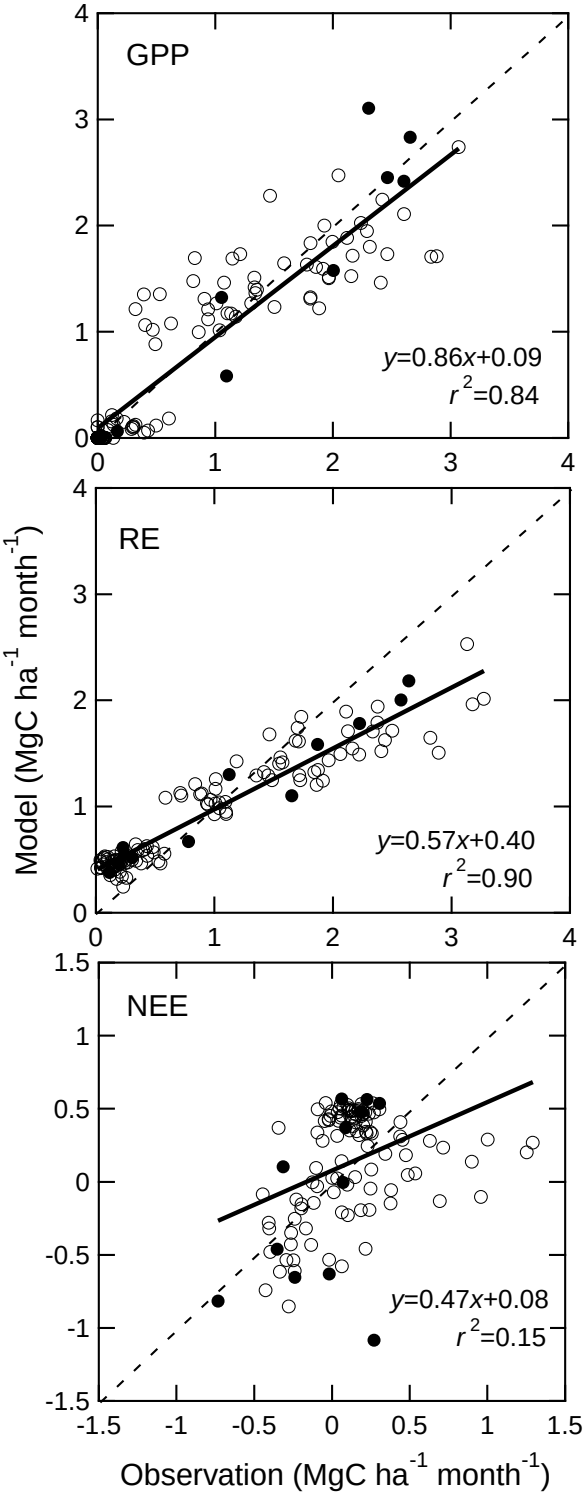
GPP
y=0.86x+0.09
r 2=0.84
RE
y=0.57x+0.40
r 2=0.90
NEE
y=0.47x+0.08
r 2=0.15
Model (MgC ha-1 month-1)
Observation (MgC ha-1 month-1)

998 **Fig. 7**

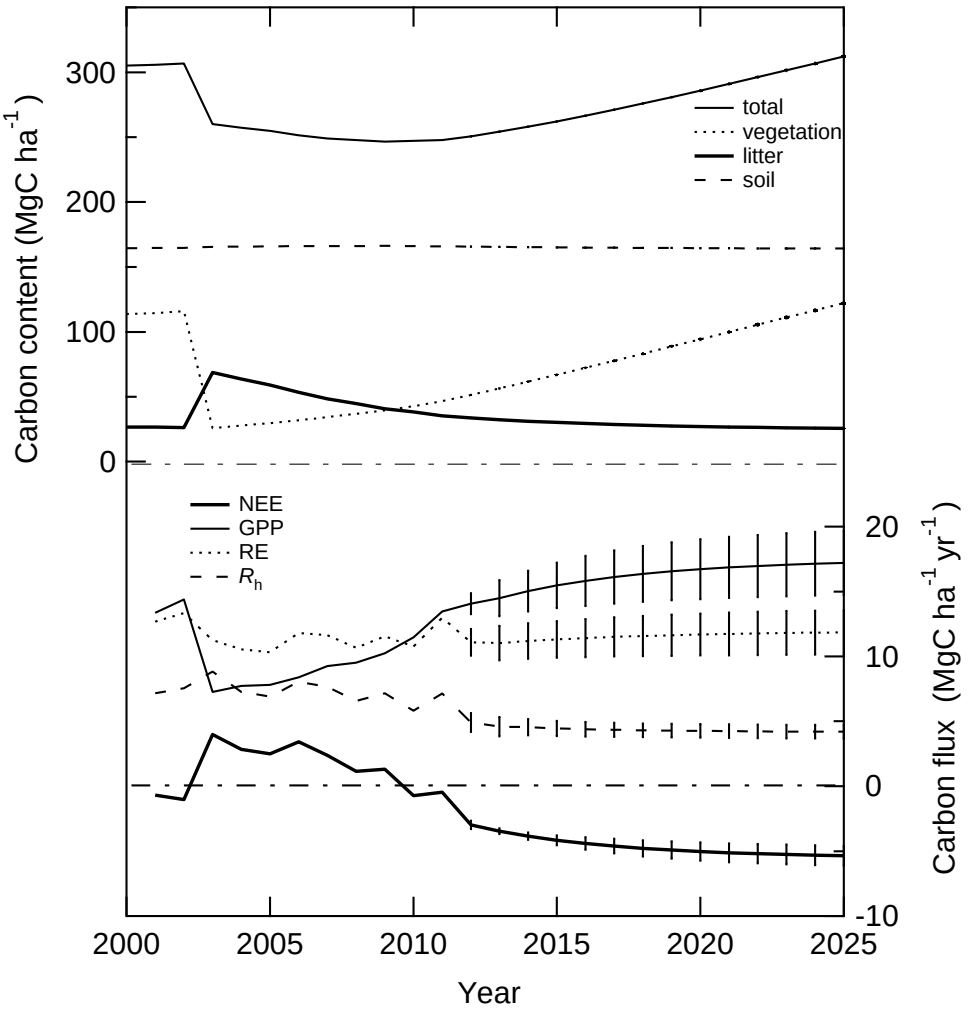
Carbon content (MgC ha-1)
300
200
100
0
total
vegetation
litter
soil
NEE
GPP
RE
Rh
20
10
0
-10
Carbon flux (MgC ha-1 yr-1)
2000
2005
2010
2015
2020
2025
Year